R-06-66

Near-surface hydrogeological model of Laxemar

Open repository – Laxemar 1.2

Emma Bosson, Svensk Kärnbränslehantering AB

July 2006

Svensk Kärnbränslehantering AB
Swedish Nuclear Fuel
and Waste Management Co
Box 5864
SE-102 40 Stockholm Sweden
Tel 08-459 84 00
+46 8 459 84 00
Fax 08-661 57 19
+46 8 661 57 19

ISSN 1402-3091
SKB Rapport R-06-66

Near-surface hydrogeological model of Laxemar

Open repository – Laxemar 1.2

Emma Bosson, Svensk Kärnbränslehantering AB

July 2006

Abstract

This report presents the methodology and the results from the modelling of an open final repository for spent nuclear fuel in Laxemar. Thus, the present work analyses the hydrological effects of the planned repository during the construction and operational phases when it is open, i.e. air-filled, and hence may cause a disturbance of the hydrological conditions in the surroundings. The numerical modelling is based on the conceptual and descriptive model presented in the version 1.2 Site Descriptive Model (SDM) for Laxemar /SKB 2006/. The modelling was divided into three steps. The first step was to update the L1.2 version model for hydrology and near surface hydrogeology /Werner et al. 2005b/, the main updates were related to the hydraulic properties of the bedrock and the size of the model area. The next step was to describe the conditions for the introductory construction by implementing the access tunnel and shafts to the model. The third step aimed at describing the consequences on the surface hydrology caused by an open repository. A sensitivity analysis that aimed to investigate the sensitivity of the model to the properties of the upper bedrock and the properties in the interface between the Quaternary deposits and the bedrock was performed as a part of steps two and three.

The model covers an area of 19 km^2. In the Quternary deposits, the surface water divides are assumed to coincide with the groundwater divides, thus a no-flow boundary condition is used at the horizontal boundaries. The transient top boundary condition uses meteorological data gathered at a local SKB station at Äspö during 2004. The bottom boundary condition and the horisontal boundary condition in the bedrock is a steady state head boundary condition taken from the open repository modelling of the bedrock performed as a parallel activity with the modelling tool DarcyTools /Svensson 2006/. The vertical extent of the model is from the ground surface to 150 m below sea level. Since the repository will be built at 450 m below sea level, it is only the upper part of the tunnel and shafts that are explicitly included in the modelling.

The groundwater modelling was performed with the MIKE SHE code, a process-based modelling tool that calculates the groundwater flow in three dimensions. It takes the whole hydrological cycle into consideration and describes the water flow from rainfall to river flow. The MOUSE-SHE coupling was used to implement the tunnel. MOUSE-SHE is a code primarily developed for urban hydrology, mainly to calculate inflow of water to sewers. The tunnel was described as a number of water pipes in MOUSE and the inflow of water from MIKE SHE to MOUSE, i.e. the flow of water from the aquifer to the tunnel, was calculated. The shafts were described as cells with atmospheric pressure.

The results from the updated MIKE SHE model for undisturbed condition agrees with the results for the L1.2 MIKE SHE model presented in /Werner et al. 2005b/. The average specific runoff from the model was calculated to 188 mm and the total evapotranspiration was calculated to 474 mm. The groundwater table in the area is shallow; the mean depth to the groundwater table was calculated to 0.7 m below ground surface. The discharge in the water courses is transient during the year and is dependent on the weather conditions.

The head drawdown and the size of the influence area are highly dependent on the level of grouting on the access tunnel and the deposition tunnels. Three levels of grouting were tested: no grouting, grouting corresponding to $K = 1 \cdot 10^{-7}$ m/s and $K = 1 \cdot 10^{-9}$ m/s. “The worst case scenario” when no grouting is used, leads to an influence area of 1.6 km^2 during the introductory construction. When the repository is implemented in the model, the repository walls have to be grouted to avoid numerical instabilities. No results have been presented

for the case with no grouting when the repository is included in the modelling. When the highest level of grouting is applied to the repository walls, the influence area is calculated to 9.2 km^2. The effects are concentrated to the tunnel constructions. The inflows to the tunnel, above 150 m below sea level, are in the same range for all levels of grouting. The inflows vary between 4–6 l/s depending on the applied level of grouting. There is good agreement between MIKE SHE and the DarcyTools model of the open repository. The calculated inflows to the repository in DarcyTools are in the same range as the sum of water leaving the model via MOUSE and over the bottom boundary in MIKE SHE. The agreement is best for the cases where the highest level of grouting is applied to the tunnel walls.

The runoff from the water courses in the area decreases because of the repository. The largest decrease is noticed in the catchment area underlain by the largest part of the repository, which also is the same catchment area as where the access tunnel is placed. The runoff from this area is reduced by 60% when the highest level of grouting is applied. No visible effects have been noticed concerning the lake water levels in the area. The only lake in the model area, lake Frisksjön, is underlain by thick layers of clay. This clay layer seems to prevent a lowering of the water level in the lake.

The results are very sensitive to the properties of the QD/bedrock interface. A low permeable layer in the interface between the bedrock and the Quaternary deposits has large consequences for the size of the influence area and the dimension of the lowering of the water table. A low permeable layer with a K-value = $1 \cdot 10^{-8}$ m/s reduces the influence area by almost 70%.

Sammanfattning

Denna rapport ger en presentation av metodiken och resultaten från modelleringen av ett öppet förvar i Laxemar. Det huvudsakliga syftet var att beskriva effekterna av tillfartstunneln, det öppna slutförvaret och hiss- och luftschakt på den ytnära hydrologin. Den numeriska modelleringen baseras på den konceptuella/deskriptiva modellen som presenteras i den preliminära platsbeskrivande modellen för Laxemar, version 1.2 /SKB 2006/. Modelleringen har delats in i tre huvuddelar. Första delen bestod i att uppdatera modellen för hydrologi och ytnära hydrogeologi från Laxemar version 1.2 /Werner et al. 2005b/. Huvudsakliga förändringar bestod i att uppdatera den geologiska modellen för berget samt att utöka modellområdet. Nästa steg i modelleringen var att beskriva den inledande byggnationen av slutförvaret. Endast tillfartstunnel och hiss- och luftschakt implementerades i modellen. Sista steget beskriver effekterna på den ytnära hydrologin av ett helt öppet förvar. Parallellt med steg två och tre gjordes en känslighetsanalys som syftade till att undersöka modellens känslighet för det ytliga bergets egenskaper samt egenskaperna i övergången mellan jord och berg.

Modellen täcker ett område på 19 km^2. Yt- och grundvattendelare antas sammanfalla i jordlagren, därför har ett s k ”no-flow” randvillkor ansatts vid de horisontella ränderna. Övre randvillkor beskrivs med hjälp av nederbörd och potentiell avdunstning. Meteorologidata från SKB:s lokala väderstation på Äspö har använts som indata, data är taget från år 2004. På bottenranden och på de horisontella ränderna i berget är det ansatt ett tryckrandvillkor som beräknats i Öppet förvar-modelleringen för det djupa berget, modelleringen har utförts med hjälp av modellverktyget DarcyTools /Svensson 2006/. Modellen sträcker sig från markytan ner till 150 m under havets nivå. Eftersom slutförvaret planeras att byggas på ett större djup är det endast de ytliga delarna av tillfartstunnel och schakt som inkluderats i modelleringen.

Grundvattenmodelleringen har genomförts med modellkoden MIKE SHE, ett processbaserat modellverktyg som beräknar grundvattenflödet i tre dimensioner. MIKE SHE beskriver hela den hydrologiska cykeln, från nederbörd till avrinning i bäckar och vattendrag. Kopplingen MOUSE-SHE användes för att implementera tunneln i modellen. MOUSE-SHE är en modellkod som framförallt är utvecklad för urban hydrologi och den används primärt för att beräkna inläckage i ledningar. Tunneln beskrevs som ett antal ledningar i MOUSE och vattenflödet mellan MIKE SHE och MOUSE, dvs tunneln, beräknades. Hiss- och luftschakt beskrevs i modellen som celler med atmosfärstryck.

Resultaten från den uppdaterade MIKE SHE modellen, som syftar till att beskriva hydrologin i området under ostörda förhållanden, stämmer bra överens med de resultat som presenterades i /Werner et al. 2005b/. Avrinningen är beräknad till 188 mm och totala evapotranspirationen beräknades till 474 mm. Grundvattenytan i området ligger nära markytan, ”medelgrundvattenytan” i hela området för den simulerande perioden ligger 0,7 m under markytan. Flödet i områdets vattendrag är transient under året och starkt kopplat till de meteorologiska förhållandena i området.

Grundvattenavsänkningen och påverkansområdet, det område som sänks av mer än 30 cm, visade sig vara mycket beroende av vilken grad av tätning som appliceras på tunnelväggarna. Tre tätningsfall testades: ingen tätning, tätning av tunnelväggarna motsvarande en hydraulisk konduktivitet på $1 \cdot 10^{-7}$ m/s och på $1 \cdot 10^{-9}$ m/s. I det fall när ingen tätning används beräknades påverkansområdet till 1,6 km^2 under inledande drift, dvs då endast tillfartstunnel och luftschakt implementerats i modellen. När hela förvaret är beskrivet i

modellen, i form av ett tryckrandvillkor beräknat i DarcyTools, måste tunnelväggarna tätas för att undvika numerisk instabilitet i beräkningarna. På grund av detta har inga resultat redovisats för fallet med helt otätade tunnelväggar. När den högsta tätningen appliceras på tunnelväggarna, $K = 1 \cdot 10^{-9}$ m/s, fås ett påverkansområde på 9,2 km^2. Den största avsänkningen sker lokalt kring tillfartstunneln. Inflödena till tillfartstunneln är i samma härad för alla olika tätningsfall och varierar mellan 4–6 l/s. Resultaten från DarcyTools modelleringen av Öppet förvar och resultaten från MIKE SHE modelleringen överensstämmer. Det inflöde som beräknats till förvaret i DarcyTools är i samma storleksordning som det vattenflöde som går över bottenranden och lämnar modellen via MOUSE, dvs via tunneln. Resultaten stämmer bäst överens för fallet med en tätning motsvarande $K = 1 \cdot 10^{-9}$ m/s.

Avrinningen från området minskar när det öppna förvaret inkluderas i modellen. Störst påverkan har beräknats i det avrinningsområde som innehåller största delarna av förvaret. Detta avrinningsområde är också det område där ramp och fyra av sex schakt är placerade. Avrinningen i detta område minskar med 60 % (jämfört med ostörda förhållanden) när den högsta tätningen appliceras på tunnelväggarna. Sjönivån i Frisksjön, som är den enda sjön i modellområdet, påverkas inte av förvaret. Sjön är, i modellen, underlagrad av ett fyra meter tjockt lerlager. Detta lerlager förhindrar en sänkning av sjönivån.

Modellen har visat sig mycket känslig för egenskaperna i övergången jord/berg. Ett lågkonduktivt lager mellan jord och berg har stor inverkan på såväl avsänkningen som påverkansområdets storlek. Ett lågkonduktivt lager med en hydraulisk konduktivitet på $1 \cdot 10^{-8}$ m/s minskar påverkansområdet med nära 70 %.

Contents

1 Introduction

1.1 Background

The Swedish Nuclear Fuel and Waste Management Company (SKB) is performing site investigations at two different locations in Sweden, referred to as the Forsmark and Simpevarp areas, with the objective of siting a final repository for high-level radioactive waste. Data from the site investigations are used in a variety of modelling activities, the results of which are presented within the frameworks of Site Descriptive Models (SDM), Safety Assessment (SA), and Environmental Impact Assessment (EIA). Numerical modelling of water flow is one of the modelling activities performed in support of SDM, SA and EIA.

The SDM provides a description of the present conditions at the site, which is used as a basis for developing models intended to describe the future conditions in the area. In particular, model predictions of the effects of the construction, operation and long-term waste storage are of interest. The latest version of the Laxemar SDM, version 1.2 (SDM L1.2, for short), is presented in /SKB 2006/. A background report to SDM L1.2, /Werner et al. 2005b/ describes the modelling of surface hydrology and near-surface hydrogeology that was performed using the Laxemar 1.2 dataset. This description is used as a starting point for the modelling presented herein, which comprises hydrological analyses of undisturbed and open repository conditions (i.e. for "natural" conditions and during the construction and operational phases, respectively).

This report presents model results of numerical flow modelling of surface water and near-surface groundwater and the effects of an open repository at the Laxemar site which is part of the Simpevarp area.

During the construction and operational phases, there will be atmospheric pressure in the open tunnels and shafts in the repository. This will cause disturbances in the pressure field around the subsurface constructions and inflow of groundwater. The size of this inflow and its possible effects on surrounding groundwater and surface systems need to be quantified. The issues related to the effects of the open repository concern both the conditions in the repository (inflows and hydrochemical conditions) and in the surrounding environment (effects of groundwater drawdown). Thus, the open repository modelling will deliver results to both SA and EIA. The modelling presented in this report is focused on the effects on the surface hydrology and near-surface hydrogeology, i.e. on the surrounding environment and produces input primarily to the EIA activities.

1.2 Objectives

With the previous SDM L1.2 as a starting point, the present work can be subdivided into the following three parts:

1. Update of numerical flow model (enlargement of the model area and inclusion of additional site data in the model).
2. Hydrological analysis of "undisturbed" conditions (sensitivity analysis and detailed analysis of the selected base case).

3. Analysis of the hydrological effects of an open repository (effects on surface hydrology and the hydrogeological conditions in the Quaternary deposits and the upper rock.

The general objectives of the present modelling are the following:

- Develop and present an updated flow model that makes full use of the Laxemar 1.2 dataset.
- Improve our understanding of the present conditions in the Laxemar area.
- Develop and demonstrate modelling tools needed for hydrological applications within SA and EIA.
- Provide qualitative and quantitative results to be used in current SA "SR-Can" and EIA (evaluation of open repository effects) activities, and in the planning of forthcoming modelling work.

1.3 Setting

The Laxemar area is located approximately 300 km south of Stockholm, in eastern Småland within the municipality of Oskarshamn. Figure 1-1 shows the regional model area considered by the site investigation and within the site descriptive modelling, and also some lakes and water courses within and in the vicinity of this area.

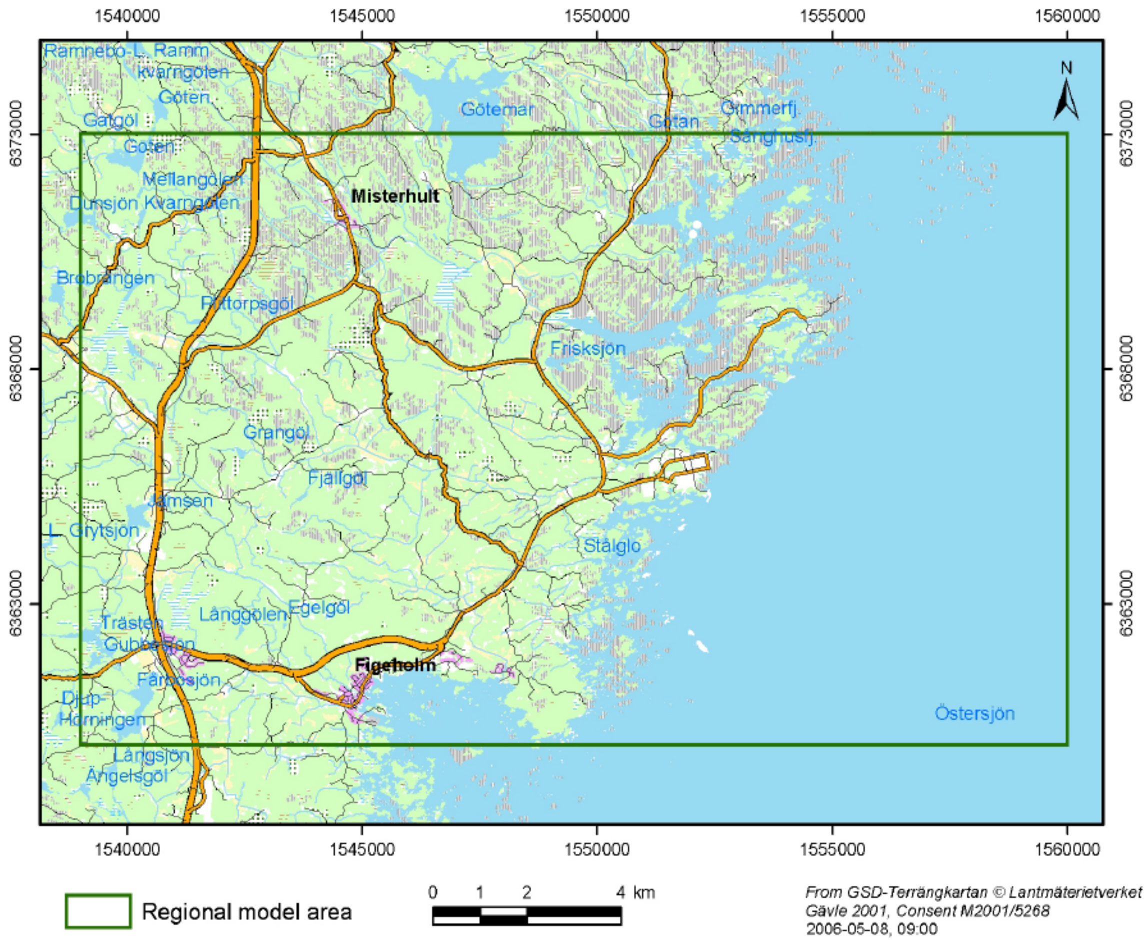

Figure 1-1. Detailed map of the land part of the regional model area and some objects of particular interest for the hydrological modelling.

As a result of the investigations and modelling performed, a further prioritisation and focusing of (some of) the investigations has been made during the course of the site investigation. Specifically, the current open repository and SA modelling uses a repository layout where the central part of the repository is located 2 km inland in the Laxemar area. A description of the climate and the hydrological and hydrogeological conditions in the Laxemar area is presented in /Werner et al. 2005b/. /Lindborg 2006/ gives a description of the whole surface and near-surface system, including the most current models of, e.g. the topography and the Quaternary deposits. The site characteristics and parameters considered in the present work are summarised and described in Chapter 2.

1.4 Modelling procedure

The modelling work has been divided into three parts. The first step was to update the MIKE SHE model from the L1.2 site descriptive modelling /Werner et al. 2005b/ with respect to model area, the channel model (M11-model) and hydraulic properties for the bedrock. A "base case" was defined in accordance to the parameter values given in Section 2.2.2. This base case was the basis for step two when tunnel and shafts were introduced into the model to investigate how these constructions will affect the near-surface hydrology in the model area. The last step was a sensitivity analysis which aimed to investigate the sensitivity to the properties in the upper bedrock and the zone between the bedrock and the Quaternary deposits. The sensitivity analysis was performed only for the open repository conditions.

1.5 Related modelling activities

Several modelling activities have provided the various external input data and models required for the present modelling and the preceding SDM L1.2 modelling. Whereas most of these inputs are described in some detail in Chapter 2 and in /Werner et al. 2005b/, we discuss here briefly the interactions with the hydrogeological activities that consider flow modelling of the integrated rock-overburden system.

This work is focused on the overburden and the upper part of the bedrock. The numerical model was developed using the MIKE SHE tool, and has a vertical extent from the ground surface to 150 m below sea level. For applications involving the repository at c 450 m below sea level as a source of a hydraulic disturbance (open repository), this means that the boundary condition at the bottom of the near-surface model preferably should be obtained from a model that includes the repository. Conversely, the larger-scale models that go down to repository depth (about twice as deep, actually) can use information from the more detailed near-surface model as a basis for setting the upper boundary condition.

The hydrogeological modelling activities that provided inputs to the various parts of this work can be summarised as follows:

- SDM L1.2 hydrological and near-surface hydrogeological modelling preformed with MIKE SHE /Werner et al. 2005b/.
- Open repository modelling Laxemar 1.2 /Svensson 2006/, delivered the hydrogeological properties of the rock and the bottom boundary condition used in the modelling of the undisturbed hydrological conditions. The model also provided the "disturbed" bottom boundary condition used in the MIKE SHE open repository simulations (the boundary condition for undisturbed conditions was also used).

1.6 This report

This report provides an integrated presentation of the modelling activities listed as parts 1–3 in Section 1.2. Chapter 2 describes the modelling tools and the input data (part 1), with emphasis on the changes since the previously reported SDM L1.2 modelling /Werner et al. 2005b/. In Chapter 3, the hydrological analysis of the undisturbed situation is reported (part 2). Chapter 4 describes the open repository simulations (part 3). Finally, Chapter 5 contains a discussion of the results, including an uncertainty evaluation, and the conclusions of the work.

2 Modelling tools and input data

2.1 Overview of modelling tools

2.1.1 MIKE SHE

MIKE SHE (Système Hydrologique Europeen) is a physically based, distributed model that simulates water flows from rainfall to river flow. It is a commercial code, developed by the Danish Hydraulic Institute (DHI). This sub-section summarises the basic processes and the governing equations in MIKE SHE. For a more detailed description, see the user's guide and technical reference /DHI Software 2004a/.

MIKE SHE describes the main processes in the land phase of the hydrological cycle. The precipitation can either be intercepted by leaves or fall to the ground. The water on the ground surface can infiltrate, evaporate or form overland flow. Once the water has infiltrated the soil, it enters the unsaturated zone. In the unsaturated zone, it can either be extracted by roots and leave the system as transpiration, or it can percolate down to the saturated zone (Figure 2-1). MIKE SHE is fully integrated with a channel-flow code, MIKE 11. The exchange of water between the two modelling tools takes place during the whole simulation, i.e. the two programs run simultaneously.

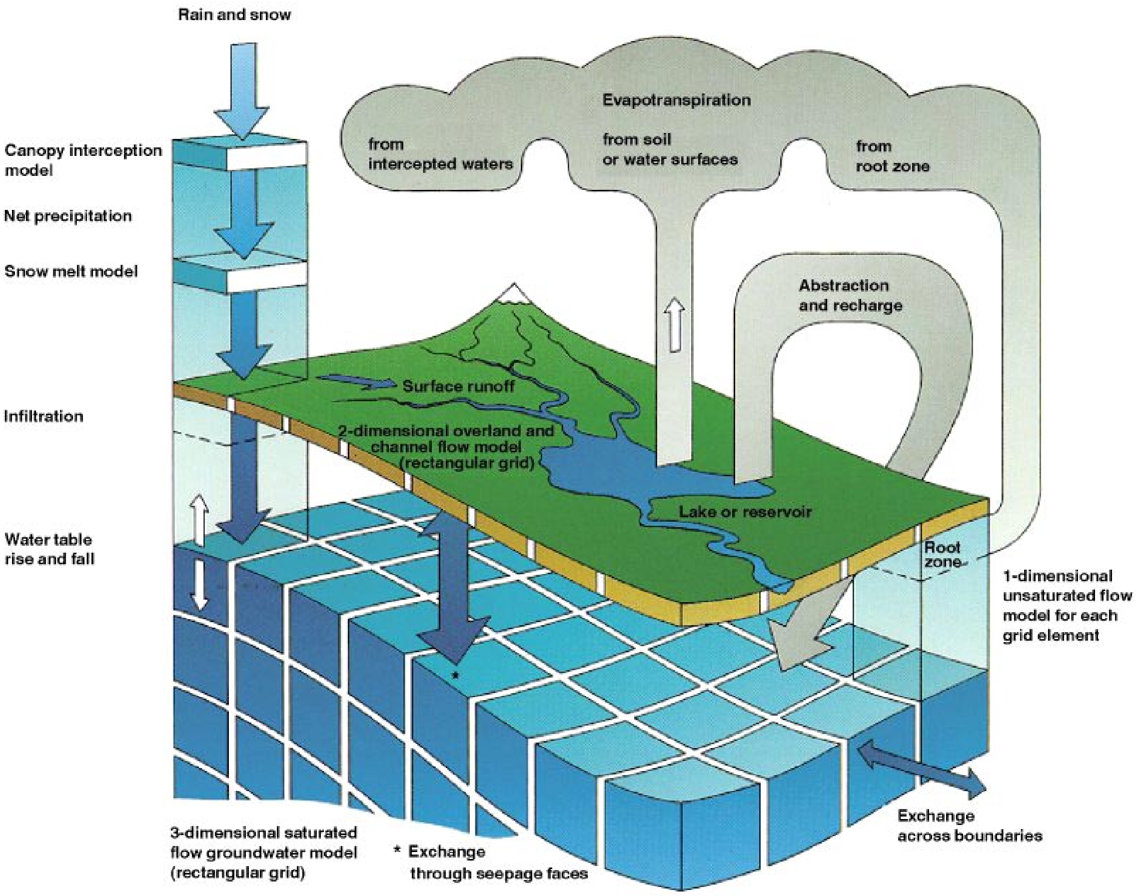

Figure 2-1. *Overview of the MIKE SHE model /DHI Sverige 1998/.*

MIKE SHE is developed primarily for modelling of groundwater flow in porous media. However, in the present modelling the bedrock is also included. The bedrock is parameterised by use of data from the Laxemar 1.2 groundwater flow model developed using the DarcyTools code /Svensson 2006/. DarcyTools uses a description of the fracture network and "intact" rock as a basis for developing an "equivalent porous medium" description that can be used by MIKE SHE.

The MIKE SHE model consists of the following five compartments:

- Overland flow (OL),
- Evapotranspiration (ET),
- Unsaturated zone (UZ),
- Saturated zone (SZ),
- Channel flow, (MIKE 11).

The water flow is calculated in different ways in each compartment. In addition to the different compartments, there is a frame component that runs simultaneously with the other components of the model. This component controls the exchange of water between all the other compartments. For a detailed description of each compartment, see /Werner et al. 2005a/ and the user's guide and technical reference /DHI Software 2004a/.

MIKE SHE version 2005 has been used within this project. The main change between this version and the version used in L1.2 is related to the calculation of plant transpiration. Version 2005 allows water uptake by plants in saturated areas. This implies that water can be extracted by plant roots even in wetland areas, which obviously is a more realistic description than in earlier versions of the MIKE SHE code. The new transpiration calculation routine is described in /Gustafsson and Vikström 2006/.

2.1.2 MOUSE-SHE

In the open repository project the program MOUSE-SHE /DHI Software 2004b/ has been used for modelling inflow to the tunnel. MOUSE-SHE is a modelling tool developed for urban hydrology. The program is primarily used for calculating groundwater infiltration to sewers. In this project the tunnel to the deep repository has been described as a number of water pipes in MOUSE. The program calculates the flow of water between the MIKE SHE groundwater model and the MOUSE model, i.e. the inflow of water to the tunnel.

A special development of the code has been performed for the present open repository modelling. The code was first applied to the Forsmark area /Bosson and Berglund 2006/. The flow from/to a MIKE SHE groundwater cell to/from a MOUSE pipe intersecting the cell is calculated as below.

$$Q_{cell} = dh \cdot L \cdot P \cdot LC$$

Q_{cell}	Leakage flow from grid cell [m^3s^{-1}]
dh	Head difference between groundwater and pipe [m]
L	Length of the section of the pipe intersecting the cell [m]
P	Wet perimeter [m] (inner – if flow from pipe to cell, outer – if flow from cell to pipe, see Figure 2-2)
LC	Leakage coefficient [s^{-1}]

When calculating the exchange of water between the groundwater program and MOUSE, the properties of the pipe and the aquifer are both taken into consideration. The "final" LC, (Figure 2-2), is calculated as a combination of the pipe leakage coefficient, $LC_{p,}$ and the "average leakage coefficient" of the grid cell in MIKE SHE, $LC_{aq,}$ as follows.

$$\frac{1}{LC} = \frac{1}{LC_p} + \frac{1}{LC_{aq}}$$

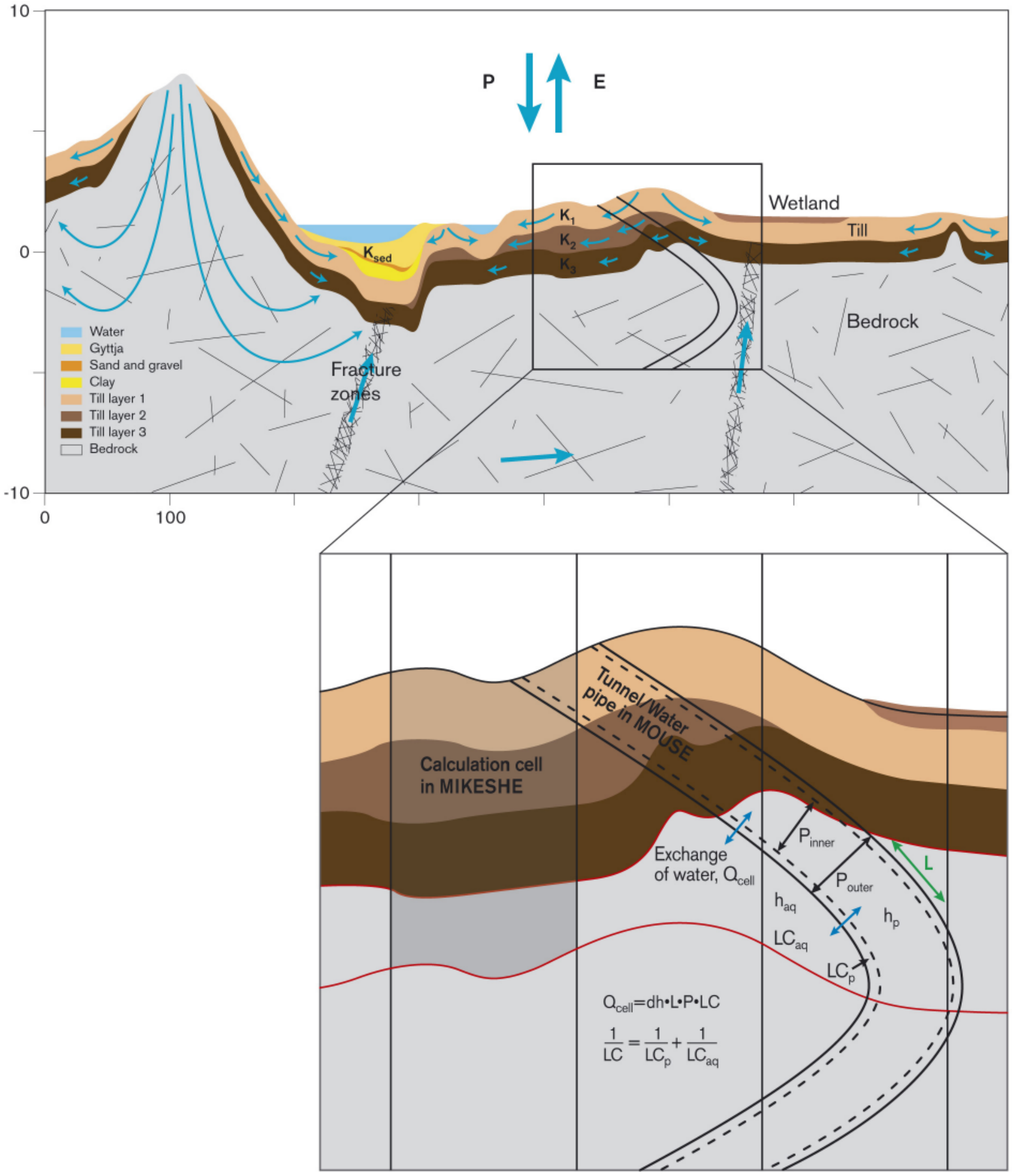

Figure 2-2. *Illustration of how the exchange of water between MOUSE and MIKE SHE is calculated.*

LC_{aq} is calculated under the assumption that the exchange water flows to/from the centre of the grid cell as horizontal and/or vertical flow. The current implementation of the MOUSE-SHE coupling does not include a detailed geometric calculation of the flow path, a MOUSE pipe can have any location in a grid cell. Instead an average flow length is used, 0.25×grid size, dx, for horizontal flow and 0.25×cell height, dz, for vertical flow. The leakage coefficient of the grid cell is calculated as below.

$$LC_{aq} = LC_{aq(h)} + LC_{aq(v)} = \frac{K_h}{0.25 \cdot dx} + \frac{K_v}{0.25 \cdot dz}$$

dx Cell size [m]
dz Cell height [m]
K_h Horizontal hydraulic conductivity [ms^{-1}]
K_v Vertical hydraulic conductivity [ms^{-1}]

LC_p is calculated as the known level of grouting, expressed as a K-value, divided by the thickness of the grouting material.

$$LC_p = \frac{K_{grout}}{d_{grout}}$$

K_{grout} Hydraulic conductivity of the grouting material [ms^{-1}]
d_{grout} Thickness of the grouting material [m]

Description of the different levels of grouting in MOUSE-SHE

Different levels of grouting were applied to the tunnel walls, the different grouting cases are described in Section 4.2. The leakage coefficients of the pipe and the aquifer are both taken into consideration when calculating the total inflow to the tunnel. The leakage coefficient for the aquifer is dependent on which calculation layer the tunnel is intersecting. As a result, the leakage coefficient for the aquifer, LC_{aq}, varies with depth and is set according to the hydraulic conductivity in the actual calculation layer. The exchange of water depends on the head difference between the tunnel and the aquifer. The only input data needed for the MOUSE-SHE simulation, except for the geometry of the tunnel, is the leakage coefficient of the tunnel wall. The tunnel ending is described as a free outlet of a water pipe, the head is set to –150 m. The MOUSE-SHE coupling is illustrated in Figure 2-2. In the cases where no grouting are applied to the tunnel walls, the leakage coefficient is set to 0.001, which is higher than that of the surrounding material; thus, it is the hydraulic properties of the aquifer that limit the inflow.

The shafts are described as cells in MIKE SHE with atmospheric pressure. The leakage of water from the aquifer to the shafts is then calculated with a total conductance, m^2s^{-1}, see below. The total conductance takes the different levels of grouting into consideration.

$$C = LC \cdot \Delta z \cdot 2 \cdot r \cdot \pi$$

$$\frac{1}{LC} = \frac{1}{LC_{aq}} + \frac{1}{LC_P}$$

$$LC_{aq} = \frac{K_h}{\Delta x}$$

$$LC_P = \frac{K_g}{l}$$

C	Conductance [m^2s^{-1}]
LC	Total leakage coefficient [s^{-1}]
LC_{aq}	Leakage coefficient of the aquifer [s^{-1}]
LC_P	Leakage coefficient of the grout [s^{-1}]
Δz	Height of calculation layer [m]
r	Radius of the shaft [m]
K_h	Horizontal hydraulic conductivity [ms^{-1}]
Δx	Grid size [m]
K_g	Hydraulic conductivity of the grout [ms^{-1}]
l	Thickness of the grouting [m]

The total conductance, for each calculation layer, used in the different cases is listed in Appendix 1.

2.2 Meteorological, hydrological and hydrogeological input data

The input data to the MIKE SHE model include data on topography, land use, geology, hydrogeology and meteorology. In addition, MIKE 11 requires information on the surface water system within the model area. The main part of the site-specific data used in this modelling is data that were available at the 1.2 data freeze for the Laxemar site, in November 2004. The MIKE SHE model used in the open repository project is based on the MIKE SHE model from the near-surface hydrology site modelling, version 1.2 for Laxemar. However, some updates have been made. The geological model of the bedrock and the hydrogeological parameters for the bedrock are based on the hydrogeological Laxemar 1.2 model, see Section 2.2.2 (bedrock geology) instead of Simpevarp 1.2. The model area was extended compared to the L1.2 MIKE SHE model and the description of the water courses was refined. A list of all the updates made in the open repository model is listed in Table 2-1. The conceptual and quantitative models that provide the basis for the MIKE SHE flow modelling in this report is described in /Werner et al. 2005b/.

Table 2-1. Changes in the present open repository model compared to the previous MIKE SHE L1.2 model.

L1.2	Open repository
Bedrock model S1.2	Bedrock model L1.2
Grid Size 20 m	Grid Size 30 m
Data from field controlled water courses in CA no 6, 7, 8, 9	Data from field controlled water courses in CA no 6, 7, 8, 9, 10 + field controlled ditches
Model area 8.9 km^2	Model area 18.88 km^2

2.2.1 Meteorology

The meteorological input data are taken from a local meteorological station established by SKB as a part of the site investigation program. Two stations have been established within the site investigation; the locations of the stations are shown in Figure 2-3. In this project data for the year 2004 from Äspö have been used. Data on temperature, precipitation and potential evapotranspiration are used in the MIKE SHE modelling. The potential evapotranspiration is calculated with the Penman-Monteith equation with data from the "Äspö" station /Werner et al. 2005b/. The annual (corrected) precipitation for the simulation period, 1 January, 2004 – 31 December, 2004, is 655 mm and the total potential evapotranspiration during this period is calculated to 434 mm.

2.2.2 Hydrogeology

The geological model and the associated parameterisation with hydrogeological parameters will be described in two parts, the Quaternary deposits and the bedrock. The input data and the model for Quaternary deposits are the same as in the MIKE SHE model for Laxemar, L1.2. The bedrock description is updated with data from the model version L1.2; in the L1.2 MIKE SHE model the bedrock model was taken from S1.2.

Quaternary deposits

Based on several types of data (e.g. data from boreholes, geophysical investigations, the QD mapping, and the DEM), a geometrical model of the overburden, in the following referred to as the "QD-model" has been developed using the ArcGIS extension GeoEditor /Nyman 2005/. In the QD-model, the overburden is divided into three main QD layers, denoted Z1–Z3 (Z1 is the top layer and Z3 the bottom layer). The model also includes three additional QD layers, referred to as M1–M3. The latter layers represent peat (M1), glaciofluvial deposits (M2) and artificial fill, i.e. deposits of bedrock material (M3; not strictly QD). In the QD-model, layer M1 replaces layer Z1 in peat areas, whereas layers M2 and M3 replace layers Z2 and Z3 in areas with glaciofluvial deposits and artificial fill, respectively. A schematic figure of the model is shown in Figure 2-4.

In the QD-model, each layer can locally have zero thickness. The total depth of QD and the thickness of each layer are assigned in grid cells. The assignment is done by interpolation of the various types of data used (see above). The thickness of each QD layer in the grid cells follows a set of "rules", depending on the total QD depth in each grid cell and the type of QD assigned to a grid cell, see /Nyman 2005/.

The QD assigned to the layers Z1–Z3 and M1–M3 in the MIKE SHE model are based on the QD-model /Nyman 2005/ and the detailed QD map /Rudmark 2004, Rudmark et al. 2005/. In Table 2-2, the QD assigned to layer Z1 is the same as to the QD defined in the detailed QD map /Rudmark 2004, Rudmark et al. 2005/. Hence, the QD in layer Z1 is based on mapping of QD in the field. The QD assigned to layers Z2 and Z3 at a certain location also depends on the QD in layer Z1, based on the conceptual-descriptive model of the QD stratigraphy in the area. Hence, the QD assigned to layers Z2 and Z3 involves a higher degree of uncertainty, as the QD stratigraphy has been observed in the field at a limited number of locations (points) by means of e.g. soil drilling.

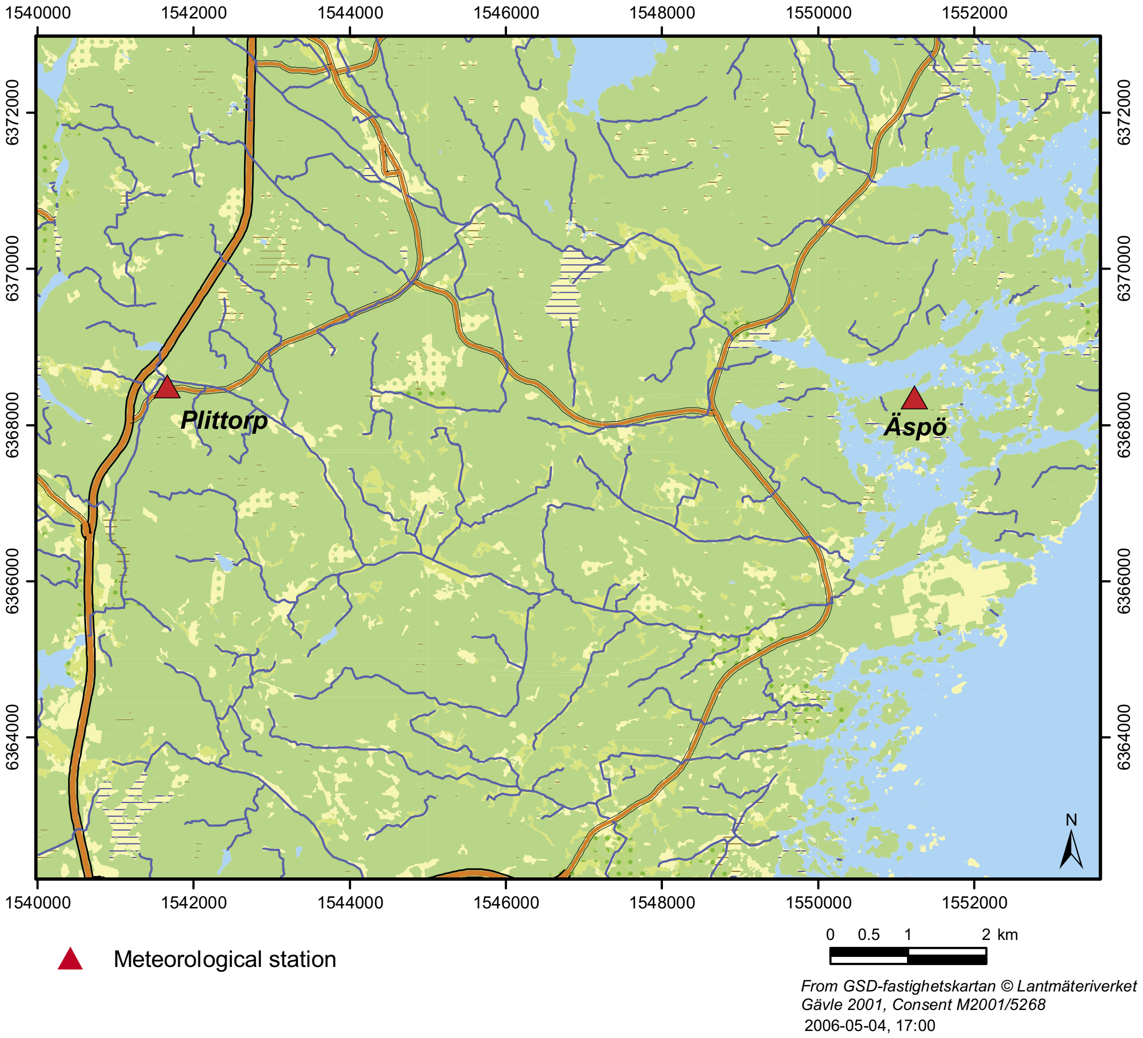

Figure 2-3. *The meteorological stations in the Simpevarp area.*

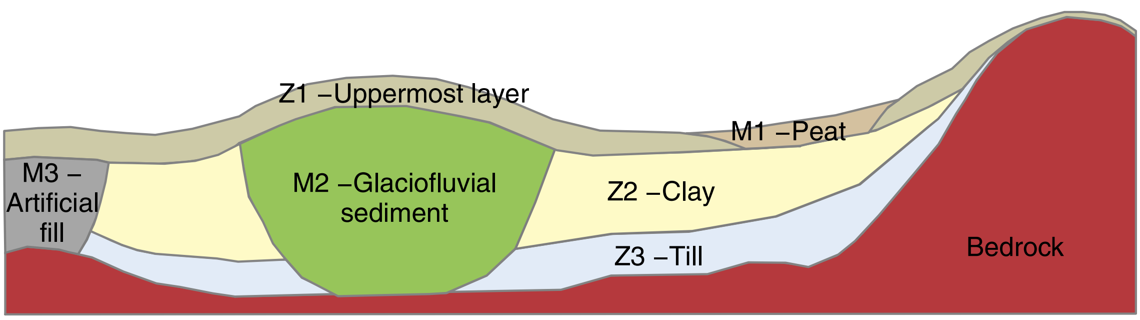

Figure 2-4. *Schematic cross section of the model of the QD-model.*

Table 2-2. Assignment of QD in layers Z1, Z2 and Z3 in the QD-model.

QD in the detailed QD map /Rudmark 2004, Rudmark et al. 2005/	QD in Z1 (layer thickness, m)	QD in Z2 (layer thickness, m)	QD in layer Z3[1]	Average total depth of QD (m)
1 – Gyttja (not on land)	Do not exist on land in the model area, assigned below open water (see 12 – Open water)			
2 – Clay gyttja, gyttja clay	Clay gyttja, gyttja clay (1.00)	2.80	Till	7.40
3 – Clay (glacial, postglacial)	Clay (1.00)	Clay (glacial 1.60, postglacial 2.80)	Till	Postglacial clay: 7.40 Glacial clay: 6.20
4 – Silt	Silt (1.00)	No Z2 layer	Till	–
5 – Till	Till (1.00)	No Z2 layer	Till	Till on land: 2.00 Till below sea: 1.00
6 – Till with thin surface layer of peat	Till (1.00)	No Z2 layer	Till	Till on land: 2.00
7 – Fluvial outwash, gravel	Gravel (1.00)	No Z2 layer	Till	–
8 – Fluvial outwash, sand	Sand (1.00)	No Z2 layer	Till	–
9 – Flood sediments, clay-gravel	Flood sediments, clay-gravel (1)	No Z2 layer	Till	–
10 – Peat (bog and fen)	Z1 is replaced by the additional layer M1 Peat (0.9)	Clay (3.80)	Till	8.30
11 – Bedrock (near-surface)	Thin soil layer, assumed to correspond to till (0.10)	No Z2 layer	No Z3 layer	0.10
12 – Open water (sea and lake)	Gyttja (0.50)	Clay (2.80 below lakes, no Z2 layer below the sea)	Till	Lake and some bays: 7.40 Sea (without QD data): 1.20
13 – Bouldery soil	Does not exist in the area considered in the flow modelling			
14 – Artifical fill	Artificial fill is assumed to correspond to till (1.00)	Z2–Z3 are replaced by the additional layer M3 Artificial fill is assumed to correspond to till		4
15 – Fluvial outwash, stones-boulders	Does not exist in the area considered in the flow modelling			
16 – Glaciofluvial deposits	Glaciofluvial deposits (1.00)	Z2–Z3 are replaced by the additional layer M2		Tuna esker: 20.00 Fårbo esker: 15.00 Other eskers (incl. the Gässhult esker: 5.00
17 – Unclassified	Till (1.00)	No Z2 layer	Till	–

[1] In the geometrical QD model, the thickness of layer Z3 below Z1 and Z2 depends on the “residual depth” down to the interpolated bedrock surface. The minmum thickness of layer Z3 is 1.00 m on land and generally 0.50 m below open water /Nyman 2005/.

The properties of the QD in the MIKE SHE model are the same as in the L1.2 MIKE SHE model. The assigned hydraulic properties of QD in the L1.2 model version are shown in Table 2-3. For a more detailed description of the hydraulic properties of the Quaternary deposits see /Werner et al. 2005b/.

Table 2-3. Assignment of hydraulic properties to QD.

QD no.	QD	Horizontal hydraulic conductivity, K_H ($m\cdot s^{-1}$)	K_H/K_V	Specific yield, S_Y (–)	Storage coefficient, S_S (m^{-1})
1	Gyttja (only present below open water)	[1] $1\cdot10^{-8}$	1	[1] 0.03	[1] $6\cdot10^{-3}$
2	Gyttja clay, clay gyttja	[2] $1\cdot10^{-7}$	1	[1] 0.03	[1] $6\cdot10^{-3}$
3	Clay (postglacial/ glacial), silt		1	[3] 0.03	[4] $6\cdot10^{-3}$
	Z1 (on land)	[4,5,6] $1\cdot10^{-6}$			
	Z2 (not in Z3)	[4,5,6] $1\cdot10^{-8}$			
4	Till, artificial fill, unclassified		1		[4] $1\cdot10^{-3}$
	Z1	[7] $4\cdot10^{-5}$		[8] 0.15	
	Z2–Z3	[7] $4\cdot10^{-5}$		[8] 0.05	
5	Fluvial outwash, gravel	[5,15] $1\cdot10^{-3}$	1	[3] 0.25	[9] 0.025
6	Fluvial outwash, sand	[5] $1\cdot10^{-3}$	1	[3] 0.25	[9] 0.025
7	Flood sediments, clay-gravel	[10] $1\cdot10^{-6}$	1	[1] 0.03	[1] $6\cdot10^{-3}$
8	Peat	[11] $1.5\cdot10^{-6}$	1	[11] 0.24	[11] $5\cdot10^{-2}$
10	Glaciofluvial deposits (coarse sand, gravel)[2]	[13] $1\cdot10^{-4}$	1	[14] 0.25	[9] 0.025

[1] Assumed equal to the corresponding parameter for clay.
[2] Assigned 10 times the K_H-value for clay.
[3] Generic data from the literature /Domenico and Schwartz 1998/.
[4] Generic data from Blomquist-Lilja, 1999 (unpublished SKB report).
[5] Generic data from the literature /Knutsson and Morfeldt 2002/.
[6] K_H for near-surface clay assigned 100 times K_H for deeper clay.
[7] Site-specific data from slug tests /Johansson and Adestam 2004b, 2004d/ and particle-size distribution curves.
[8] Based on the conceptual-descriptive model of till in the Forsmark 1.2 model /Johansson et al. 2005/.
[9] Assigned 1/10 of S_Y.
[10] Assumed to be 100 times the K_H-value for clay and 10^{-4} times the K_H-value for gravel.
[11] Generic data from the literature /Kellner 2003/.
[12] K_H and S_Y are the same as for the uppermost part of the bedrock in the DarcyTools data set (S1.2 model version), S_S is calculated based on an empirical relation between S_S and K_H in bedrock /Rhén et al. 1997, see also Chapter 5/.
[13] Assigned a value equal to 1/10 of the K_H-value for gravel.
[14] Assumed to be equal to sand and gravel.
[15] A K_H-value of $1\cdot10^{-2}$ $m\cdot s^{-1}$ may be more reasonable for gravel, but the value was decreased by 1/10 in the quantitative water flow model (Section 4.2) due to numerical instability.

In MIKE SHE, there is a separate module for modelling of unsaturated water flow. In order to reduce the simulation time, which generally is long when unsaturated water flow is to be calculated numerically, MIKE SHE performs the unsaturated zone calculations in a number of selected "type areas". Each type area represents different conditions in terms of depth to the groundwater table (divided into depth classes), type of QD, and land use (vegetation). The initial groundwater table (at the start of the simulated period), and the QD and vegetation maps are used to identify the type areas.

For each type of QD, a "typical" (layered) vertical soil profile is defined and used in the calculations. Unsaturated zone-specific hydraulic parameters are also required for each soil type included in the defined profiles. These parameters include the relationships between water content and capillary pressure head, and (unsaturated) hydraulic conductivity and water content. In the present modelling, an internal MIKE SHE database is used. This database includes these relationships for various soils in tabulated form. Based on the QD map, one typical soil profile is defined for each type of QD. Some QD types are lumped, resulting in totally 6 "type profiles". The soil profiles are described in Table 2-4 below. The individual layers within each profile are referred to as "UZ layer" 1, 2, and 3.

Table 2-4. Soil type profiles defined for modelling of unsaturated water flow in MIKE SHE. There is one soil type profile for each type of QD in the QD map (note that some QD classes are lumped into a single soil type). The numbers within brackets denote the assigned vertical extension (m b g s) for each UZ layer in the soil type profiles.

Soil type profile (QD in QD map)	UZ layer 1 (vertical extension, m b g s)	UZ layer 2 (vertical extension, m b g s)	UZ layer 3 (vertical extension, m b g s)	Comments
1 – Gyttja				Areas with gyttja only exist below open water in the MIKE SHE model area (see 12 – Water)
2 – Clay gyttja, gyttja clay	Clay (0–2.5)	(Coarse) till (2.5–20)	No UZ layer 3	Part of the lumped soil type 20 (clay/gyttja)
3 – Clay	Clay (2.5)	(Coarse) till (2.5–20)	No UZ layer 3	Part of the lumped soil type 20 (clay/gyttja)
4 – Silt				No areas with silt exist in the MIKE SHE model area
5 – Till	(Coarse) till (0–20)	No UZ layer 2	No UZ layer 3	Part of the lumped soil type 21 (till)
6 – Till with thin peat cover	(Coarse) till (0–20)	No UZ layer 2	No UZ layer 3	Part of the lumped soil type 21 (till)
7 – Fluvial outwash, gravel	Gravel (0–1)	Clay (1–4)	(Coarse) till (4–20)	Part of the lumped soil type 22 (gravel)
8 – Fluvial outwash, sand	Sand (0–5)	Clay (5–7)	(Coarse) till (7–20)	
9 – Flood sediment, clay-gravel	Clay (0–5)	(Coarse) till (5–20)	No UZ layer 3	
10 – Peat	Peat (0–1)	(Coarse) till (1–20)	No UZ layer 3	
11 – Bedrock	Till (0–20)	No UZ layer 2	No UZ layer 3	Only till is defined in the profile
12 – Water	Clay (0–5)	(Coarse) till (5–20)	No UZ layer 3	
13 – Bouldery soil				No areas with bouldery soil exist in the MIKE SHE model area
14 – Artificial fill	(Coarse) till (0–20)	No UZ layer 2	No UZ layer 3	Part of the lumped soil type 21 (till)
15 – Fluvial outwash, stones/boulders				No areas with fluvial outwash, stones/ boulders exist in the MIKE SHE model area
16 – Glaciofluvial deposits, coarse silt/boulders	Gravel (0–1)	Clay (1–4)	(Coarse) till (4–20)	Part of the lumped soil type 22 (gravel)
17 – Unclassified	(Coarse) till (0–20)	No UZ layer 2	No UZ layer 3	Part of the lumped soil type 21 (till)

Table 2-5 summarizes the unsaturated zone-specific hydraulic properties assigned to the soil types in Table 2-4, according to the internal MIKE SHE database; the required parameters include K_s, θ_s, θ_{fc}, and θ_r. The table also shows values of the specific yield, S_Y, calculated from the database values of the water content at full saturation (θ_s) and the field capacity (θ_{fc}), by use of the commonly known expression $S_Y = \theta_s - \theta_{fc}$.

Table 2-5. Unsaturated zone-specific hydraulic properties for the soil types in Table 4-5.

Soil type	Hydraulic conductivity at saturation, K_s ($m \cdot s^{-1}$)	Water content at saturation (θ_s)	Field capacity (θ_{fc})	Residual water content (θ_r)	$S_Y = \theta_s - \theta_{fc}$
Clay/gyttja	$1.0 \cdot 10^{-8}$	0.62	0.31	0.10	0.31
Sand	$4.2 \cdot 10^{-5}$	0.47	0.04	0.02	0.43
(Coarse) till	$4.0 \cdot 10^{-5}$	0.38	0.30	0.03	0.08
Peat	$1.5 \cdot 10^{-6}$	0.84	0.60	0.10	0.25
Gravel	$2.0 \cdot 10^{-3}$	0.30	0.09	0.02	0.21

For (coarse) till, peat and gravel, the calculated S_Y-values in the table agree well with those used for the saturated (groundwater) zone, cf Table 2-3 The S_Y-values for the saturated zone are found in the literature. However, it can be noted that the S_Y-values for clay/gyttja ($S_Y = 0.31$) and sand ($S_Y = 0.43$) in the table are higher than those used for the saturated zone. For the saturated zone, the corresponding values are 0.03 and 0.25. In order to keep the model numerically stable, till is assigned in the whole "type profile" in areas with shallow/exposed bedrock.

Bedrock

Modelling results and the associated input data required for the bedrock in the MIKE SHE model are taken from the open repository model for the "deep bedrock", performed in the modelling tool DarcyTools /Svensson 2006/. The data used in that modelling are based on data from the L1.2 model of the hydraulic properties of the bedrock /SKB 2006/, as presented by the ConnectFlow modelling team. However, these data comprise horizontal and vertical hydraulic conductivities and effective porosities only. Hence, data on the specific yield (S_Y) and the specific storage coefficient (S_S) are not included in the provided DarcyTools data set. As an approximation, the S_Y of the bedrock is in the present modelling assumed to be equal to the effective porosity, whereas the specific storage coefficient S_S (m^{-1}) of the bedrock is calculated according to the empirical relationship described below /Rhén et al. 1997/.

$$S_S = a \cdot K_h^{\,b}$$

In this equation, a fit to experimental data from the Äspö Hard Rock Laboratory has provided the values

$a = 6.037 \cdot 10^{-5}$

$b = 0.2312$

The properties are varying throughout the vertical profile. The bedrock is divided into 30 m thick layers. The horizontal resolution of the properties is varying, a detailed grid, 30×30 m^2, is applied in the area underlain by the repository. Outside the repository area the resolution is 100 m. The horizontal hydraulic conductivity of the bedrock at 150 m below sea level is presented in Figure 2-5. The fracture zones are shown as high conductive areas. For a more detailed description of the bedrock properties see /Svensson 2006/ and /SKB 2006/.

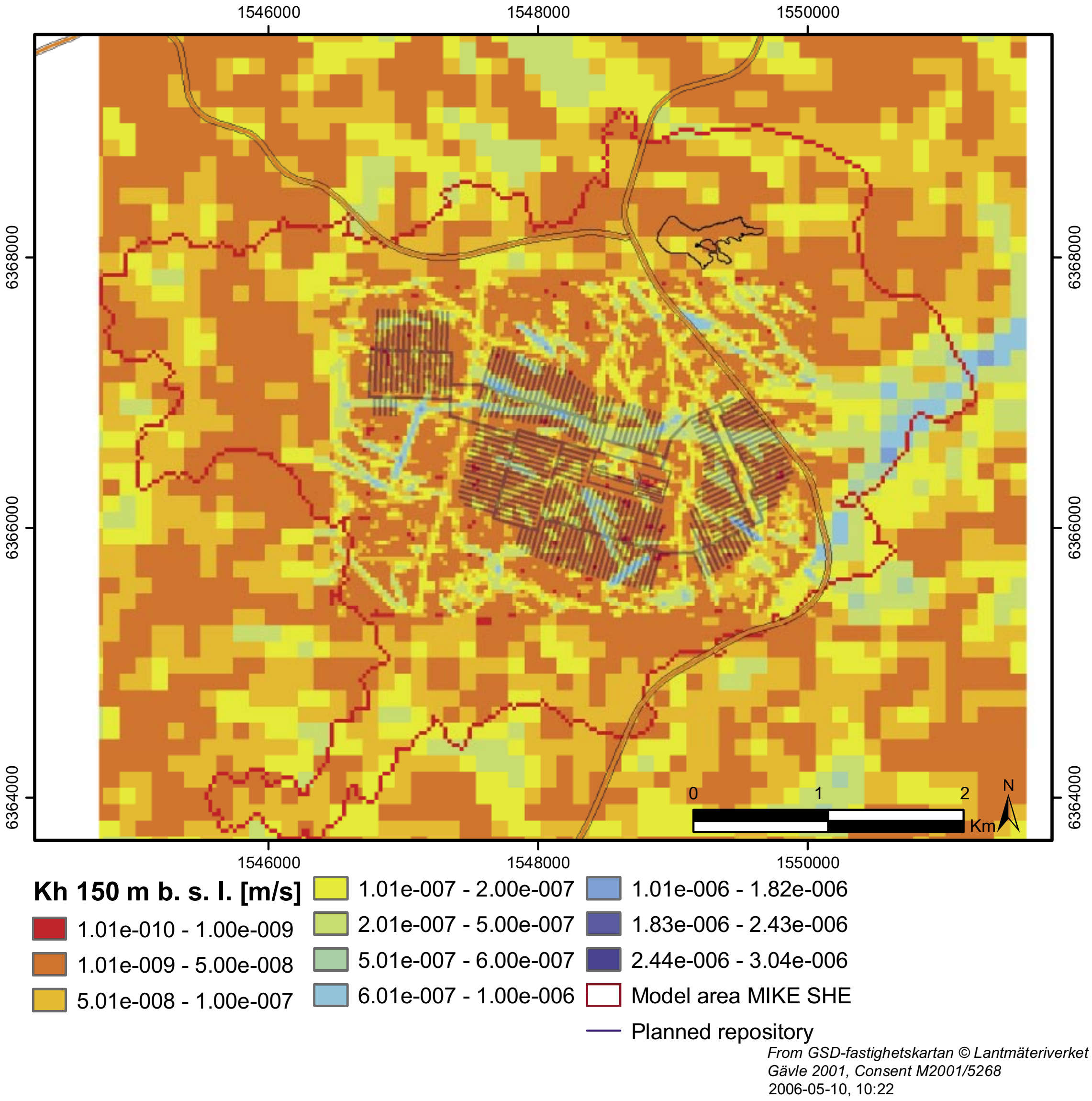

Figure 2-5. *The horizontal hydraulic conducitivity at 150 m below sea level, the planned repository and the MIKE SHE model area are also marked in the figure.*

2.2.3 Water courses

The MIKE 11 (stream network) model requires geometrical information on the water courses, including their positions in the horizontal plane, bottom levels, and cross sections. A description of the main water courses was presented by /Strömgren et al. 2006/. /Bosson and Berglund 2005/ identify drained areas in the Laxemar area. The ditches identified in that investigation are included in the MIKE 11 model. The water courses where the cross section and the bottom elevations have been measured in the field are presented in Figure 2-6. The figure also shows the field controlled ditches described in /Bosson and Berglund 2005/ and the ditches identified from aerial photos. Water courses not included in the measurements are assumed to have a triangular shape with a width of 2 m and a depth of 1 m.

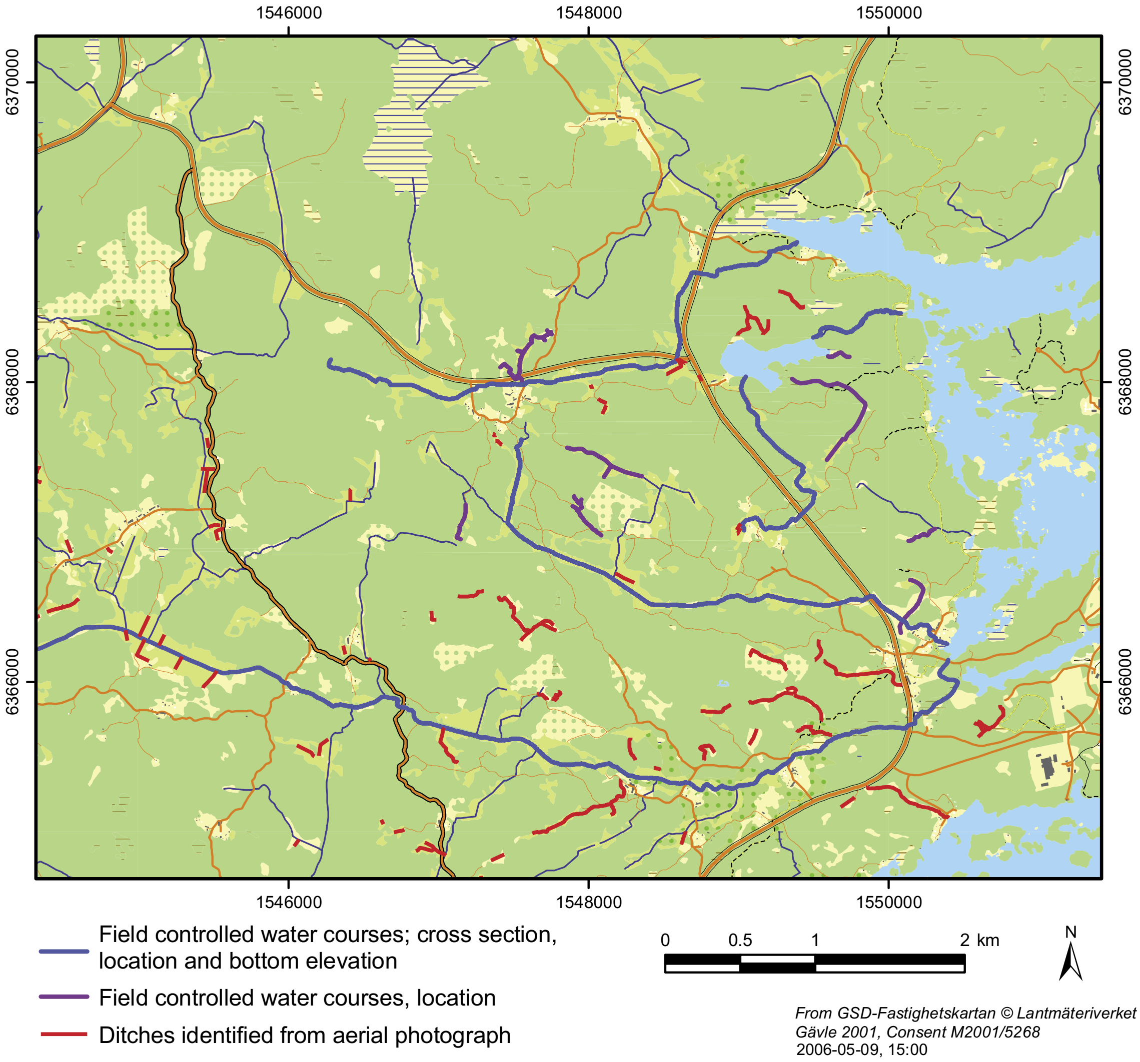

Figure 2-6. *Field controlled cross sections in the water courses and field controlled ditches in the Laxemar area.*

2.2.4 Vegetation

Land use is incorporated in the model by the vegetation map of the Simpevarp area /Boresjö Bronge and Wester 2003/. Five land use (vegetation) types are defined in the model area: deciduous forest, mixed forest, coniferous forest, water, and grass areas. The classification is made based on tree-layer data extracted from the vegetation map; areas assigned the class "no tree layer" in that map are classified as grass areas. Each vegetation type is assigned vegetation-specific parameters, required for the interception-evapotranspiration calculations in MIKE SHE. The parameters required are the leaf area index (LAI), the crop coefficient (K_c), and the root depth. For a more detailed description of the evapotranspiration calculation parameters see /Werner et al. 2005b/ where also a sensitivity analysis of these parameters is presented.

3 Modelling of undisturbed conditions

The modelling work has been divided into three parts. The first step, to update the MIKE SHE model from the L1.2 site descriptive modelling /Werner et al. 2005b/ with respect to model area, the M11-model and hydraulic properties for the bedrock is described in this chapter. A "base case" was defined in accordance to the parameter values given in Section 2.2.2.

3.1 Description of the numerical model and initial base case

3.1.1 Boundaries and grid

The model area (domain in 3D) includes catchment areas 6–9 and some sub-catchments of catchment area number 10, Laxemarån. The associated coastal land and sea areas, i.e. areas with direct runoff to the sea and the sea bottom some distance into the adjacent bay of the Baltic are also included in the model area, see Figure 3-1.

The horizontal spatial resolution of the model is 30 m, whereas the vertical discretisation of the calculation layers follows that of the geological (QD) layers Z1–Z3 and M1–M3 (cf Section 2.2.2). The ground surface, as given by the topographic model, is the upper model boundary, and the bottom boundary of the model is at 150 m below sea level.

The groundwater divides are assumed to coincide with the surface water divides. Thus, a no-flow boundary condition is used for the on-shore part of the model boundary. The sea forms the uppermost calculation layer in the off-shore parts of the model. Since large volumes of overland water can cause numerical instabilities, the sea is described as a geological layer consisting of highly permeable material. The hydraulic conductivity of this material is set to 0.001 ms^{-1}. The sea part of the uppermost calculation layer has a fixed head boundary condition, with the head set to 0 m below sea level.

The top boundary condition is expressed in terms of the precipitation and potential evapotranspiration. The precipitation is assumed to be uniformly distributed over the model area, and is given as a time series. The boundary condition for the saturated zone is described by the processes in the unsaturated zone. Water is extracted from the model volume by the "river network" modelled by the MIKE 11 model. The amount of water flowing to the channel flow model, MIKE 11, depends on the conditions in the other compartments of the model. Water is transported to the water courses via overland flow, and from the saturated zone.

The bottom boundary condition is a fixed-head condition. Model results from the "deep" hydrogeological open repository modelling, performed with DarcyTools, are used as input data when setting the bottom boundary condition. The calculated hydraulic head from 150 m below sea level is imported to the MIKE SHE model. The time step used in the Darcy Tools simulations (one year) is much longer than that in the MIKE SHE modelling, which implies that short-term temporal variations cannot be captured. Thus, the bottom boundary condition in the MIKE SHE model is assumed to be constant in time.

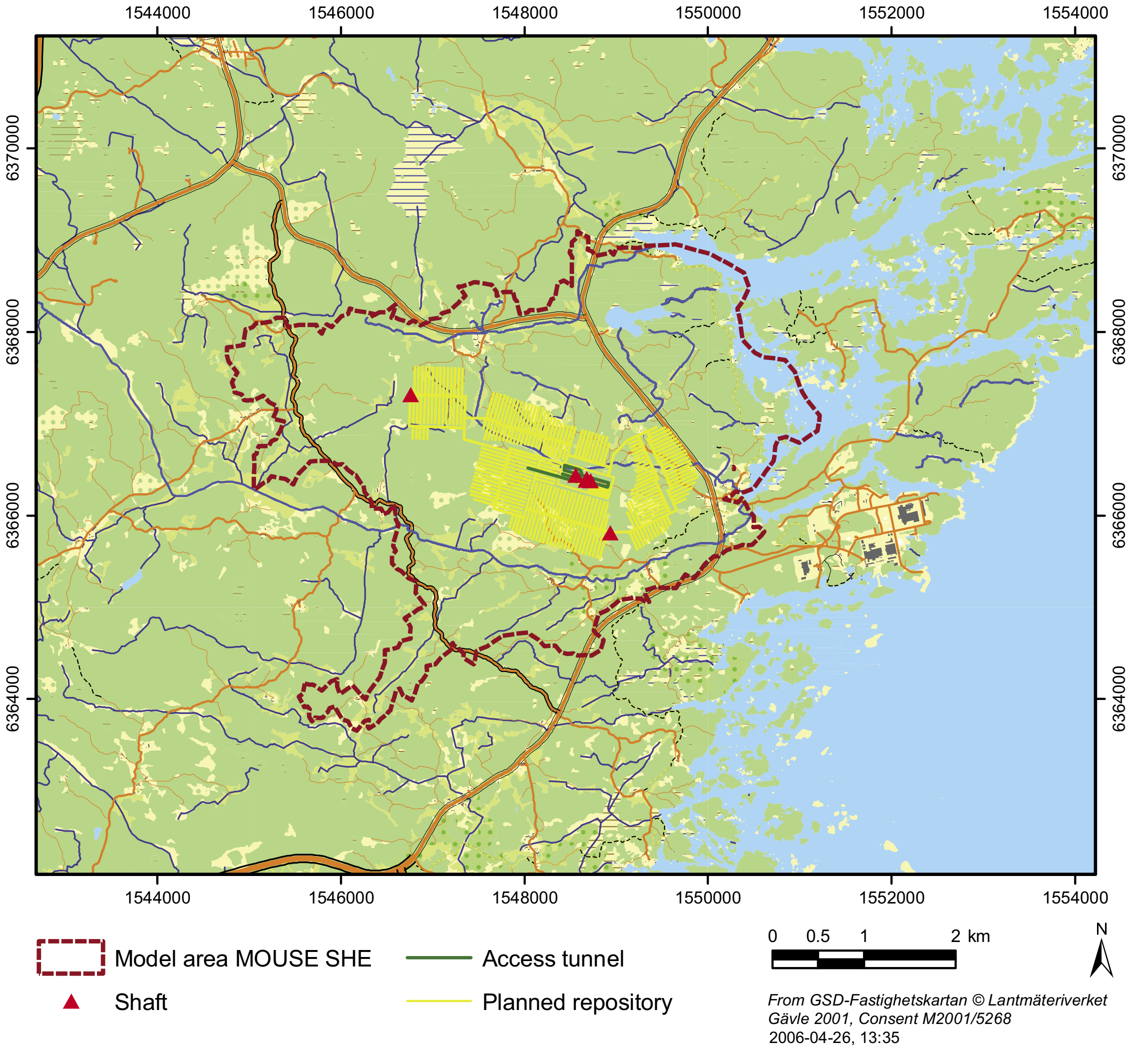

***Figur 3-1.** The model area in the present MIKE SHE modelling of the Laxemar site.*

3.1.2 Initial condition and handling of temporal variations

The simulations have been performed using meteorological input data for the one-year period from January 2004 to December 2004. Locally measured data on the meteorological parameters are available for this period; this is the main reason for the choice of simulation period.

A so-called "hot start" was used to generate the initial conditions of the model. In the base case simulation, the model was run until semi steady-state conditions were reached. This means that the model was run, with the time-dependent boundary conditions given by the meteorological data, until the variations during the year had stabilised (e.g. the pressure at a certain point shows more or less the same variation from one year to the next). The results from this simulation were used as initial conditions for the one-year simulation used to generate the final simulation results.

3.2 Results for undisturbed conditions

This chapter gives a short presentation of the results for undisturbed conditions. The natural conditions are needed as a reference to the simulations where the tunnel and shafts have been implemented in the model. The presentation includes calculated water balances, surface water discharges, and groundwater levels. It should be noted that no calibration has been performed.

3.2.1 Water balance

The water balance presented here represents a sub-volume within the total model volume. Since the sea is represented as a highly conductive geological layer with a fixed head, the sea and the model volume covered by the sea are not included in the water balance calculations (Figure 3-2). Thus, the arrows in Figure 3-3 represent the flow of water that crosses the boundary to the sea.

The calculated water balance is presented in Figure 3-3. The figure presents the flow of water between the different land compartments in the model, (the sea and the model volume under the sea are not represented in the water balance calculations). All water balance components are expressed as area-normalised total volumetric discharges, i.e. in mm (which is equivalent to mm/year in this case). The accumulated precipitation during the modelled period is 655 mm. The total evapotranspiration is calculated to 474 mm. The total evapotranspiration is the sum of the evaporation from snow (3 mm), evaporation from interception (183 mm), evaporation from ground surface (5 mm) and the upper soil layers (53 mm), transpiration from plants (203 mm) and evaporation from the saturated zone (27 mm) (see Figure 3-3). Most of the water turnover takes place in the upper part of the soil profile. The processes related to evapotranspiration all take place in the uppermost calculation layer. The total amount of water that leaves the model volume during the simulation period is 188 mm. The water that discharges via water courses and as direct run-off to the sea is 181 mm, the remaining 7 mm that leaves the model volume is groundwater discharge from the saturated zone. The groundwater recharge from the unsaturated zone to the saturated zone is 126 mm. Most of the water in the saturated zone exchanges water with the river and the overland part of the model.

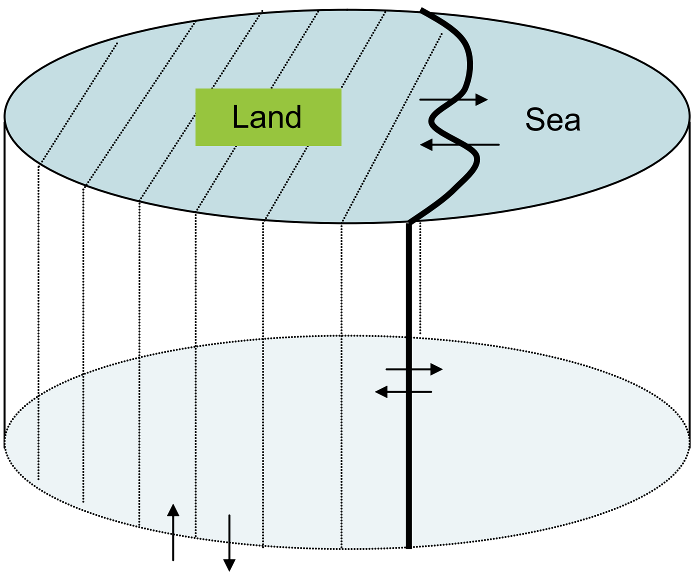

Figure 3-2. *Sub-area for the water balance calculations. The water balance is only calculated for the part of the model volume where there is land at the surface.*

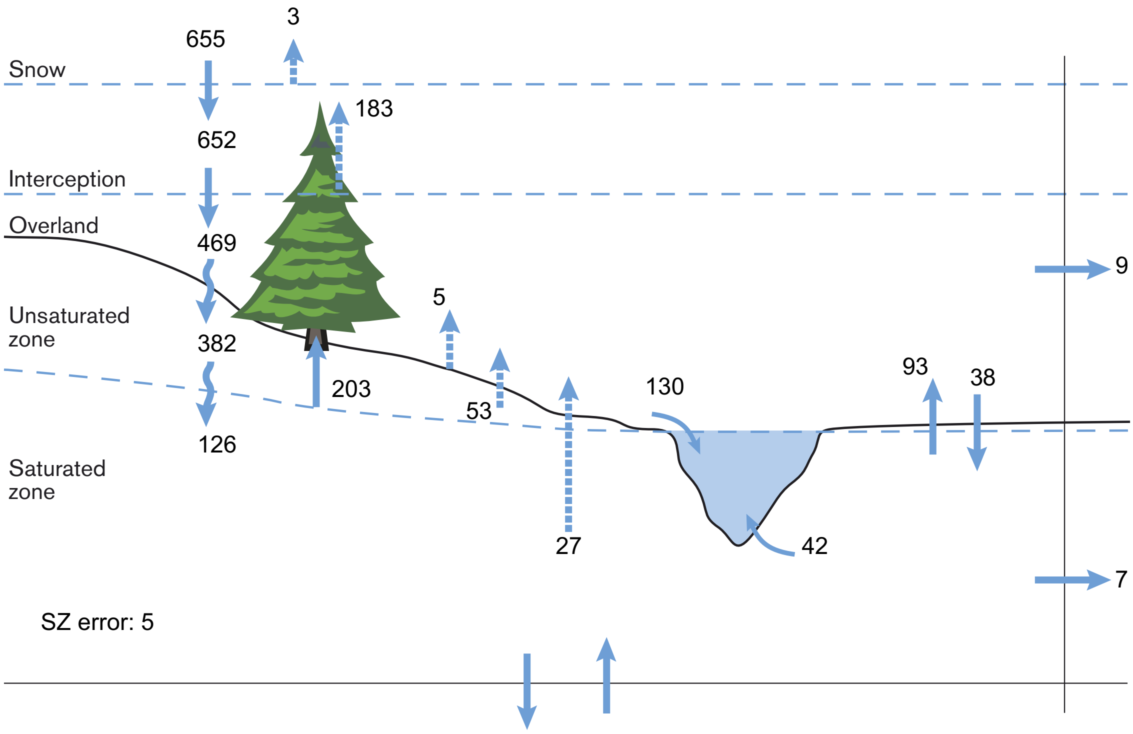

***Figure 3-3.** Calculated water balance for the Laxemar area [mm].*

The results agree with the L1.2 results presented in /Werner et al. 2006/. In L1.2 the total run-off was calculated to 189 mm and the total evapotranspiration was calculated to 466 mm per year. The largest difference between the two models concerning the water balance is the difference in the fractions of the total evapotranspiration. Since plant roots are allowed to extract water even in ponded areas, the total area with ponded water is smaller in the open repository model than in the L1.2 MIKE SHE model. The evaporation from ponded areas is accordingly less in the Open repository model than in the L1.2 MIKE SHE model since the amount of water available for evaporation from ponded areas has decreased. On the other hand, the amount of water that evaporates from the saturated zone increases in the Open repository model, which results in almost the same total evapotranspiration for the two models. Updates in the M11 model, i.e. the new field controlled data for cross sections and locations and the introduction of an additional water course, Laxemarån, resulted in a larger transport of water from the saturated zone to M11. However, the direct run-off from Overland to the sea and the groundwater run-off from the saturated zone is smaller which results in the same total run-off for the two models.

3.2.2 Discharge in water courses

As described above, the runoff is calculated as the net flow of water to the MIKE 11 model plus the water that leaves the model area as overland flow and groundwater flow. MIKE 11 calculates the discharges and water levels in the water courses. The calculated discharge in a water course varies during the year. This is illustrated in Figure 3-4, which shows the hydrograph calculated for Laxemarån in three different cross sections along the water course. As shown in the figure, the discharge is higher at downstream observation points. It can also be noted that the peaks in the discharge occur more or less simultaneously. The calculated hydrograph in the water course is transient during the year, i.e. it has several marked peaks and periods of low flow rates between the peaks. The calculated discharge from all the water courses in the model area during the year 2004 was calculated to 172 mm (cf Figure 3-3), which corresponds to 5.5 l/s · km^2.

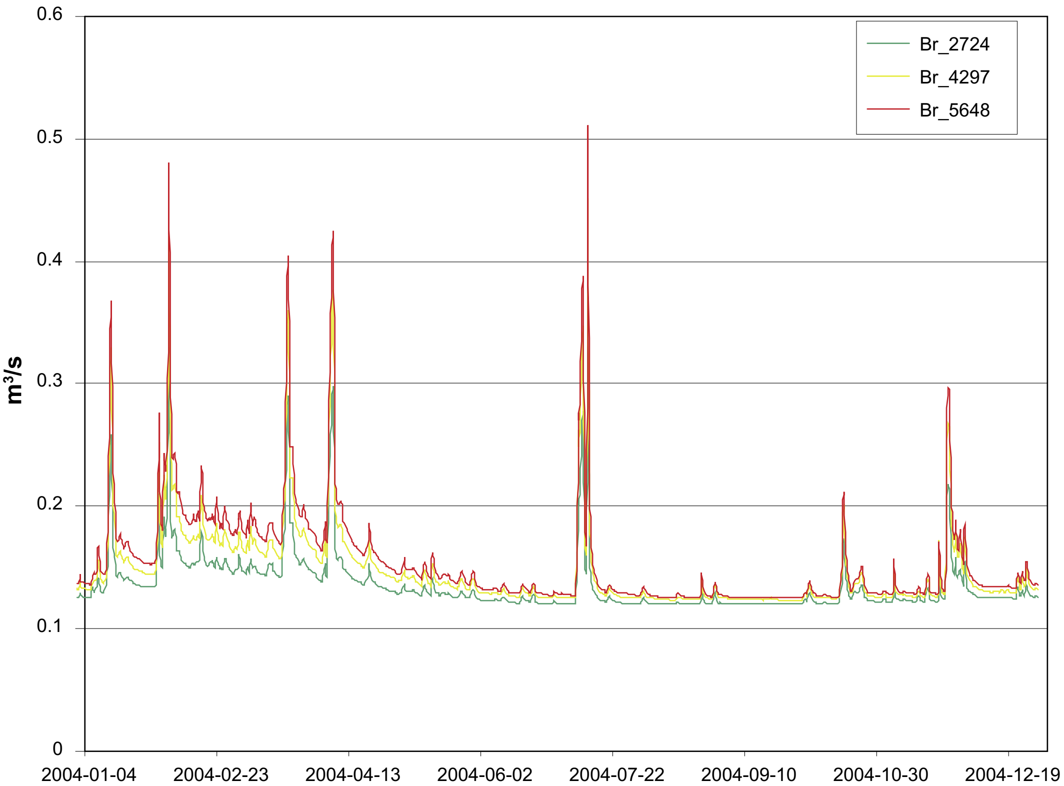

Figure 3-4*. Calculated discharge in Laxemarån at different locations from the start of the water course in M11, Br_2724 is the most upstream observation point.*

These results indicate that the flow is highly dependent on the weather conditions. The maximum discharge occurs in the middle of the summer, during a period of intensive rain. It should be noted that Figure 3-4 is just one example of the results from the MIKE 11 model; discharges and water levels in all points along the water courses are available as outputs from the modelling. In future model versions such results will be compared with measured water levels and discharges (presently no data are available from the hydrological stations in the water courses).

3.2.3 Groundwater table

Figure 3-5 shows the annual average depth to the groundwater table in the model area, as calculated for the undisturbed conditions. As can be seen in the figure, the groundwater table is shallow and located less than 2 m below ground in most of the model area. The deeper groundwater levels are mainly found in high-altitude areas, associated with groundwater recharge near the groundwater divides. There are also areas with a groundwater pressure head above the ground surface. Hence, these are groundwater discharge areas, including e.g. Lake Frisksjön and areas in the vicinity of the main water courses, i.e. (local) low-altitude areas according to the DEM /Brydsten and Strömgren 2005/. The mean depth to the groundwater table in the model area (except from the sea) for the simulated year is 0.7 m.

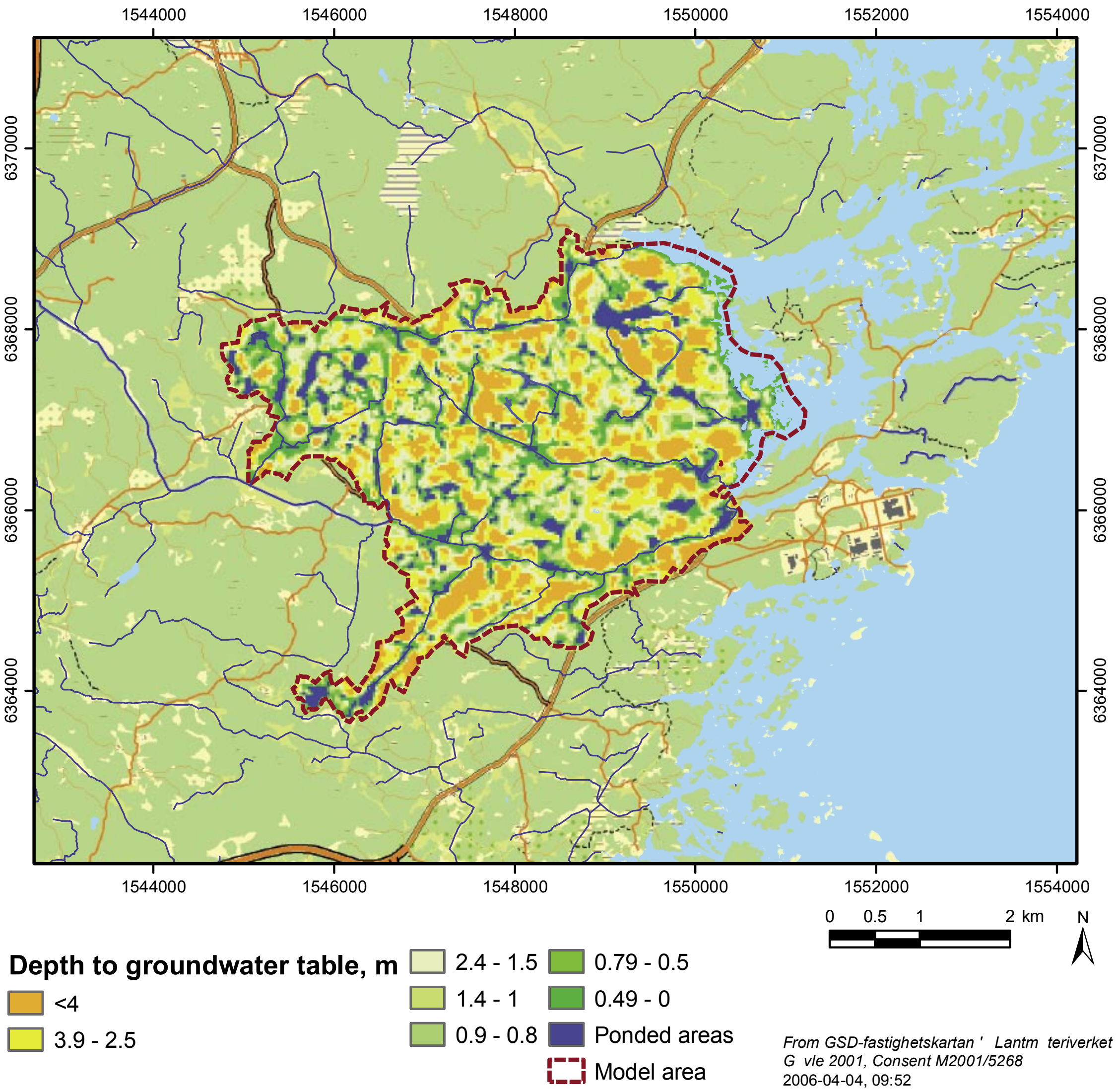

***Figure 3-5.** Mean calculated groundwater table for the simulated year 2004.*

4 Hydrological analysis of open repository conditions

The main objective with this part of the work is to analyse the surface system responses to an operational phase repository. The aims of the modelling described in this chapter are to:

- Describe the surface system under disturbed conditions.
- Predict the inflows to the tunnel and shafts for different levels of grouting.
- Quantify the near-surface drawdown caused by the tunnel and shafts.
- Describe the impact of the tunnel and shafts on lake water levels and discharges in water courses.

4.1 Geometry of the tunnel and shafts

The layout of the tunnel and the shafts are shown in Figure 4-1. The values at each curve of the tunnel give the elevation, m a s l. The radius for each shaft is also given in the figure, the circumference of the tunnel is approximately 20 m. There are totally six shafts, two of them are not visible in Figure 4-1 because of their location. These shafts are not placed in the central area of the repository. The tunnel is described as a number of links in the modelling tool MOUSE (Section 2.1.2). The six shafts are described as cells with atmospheric pressure in MIKE SHE (see Section 2.1.2) It is only the upper parts of the construction that are described in the MOUSE-SHE model, the extent of the tunnel is the same as the extent of the groundwater model, i.e. the tunnel ends at 150 m below sea level.

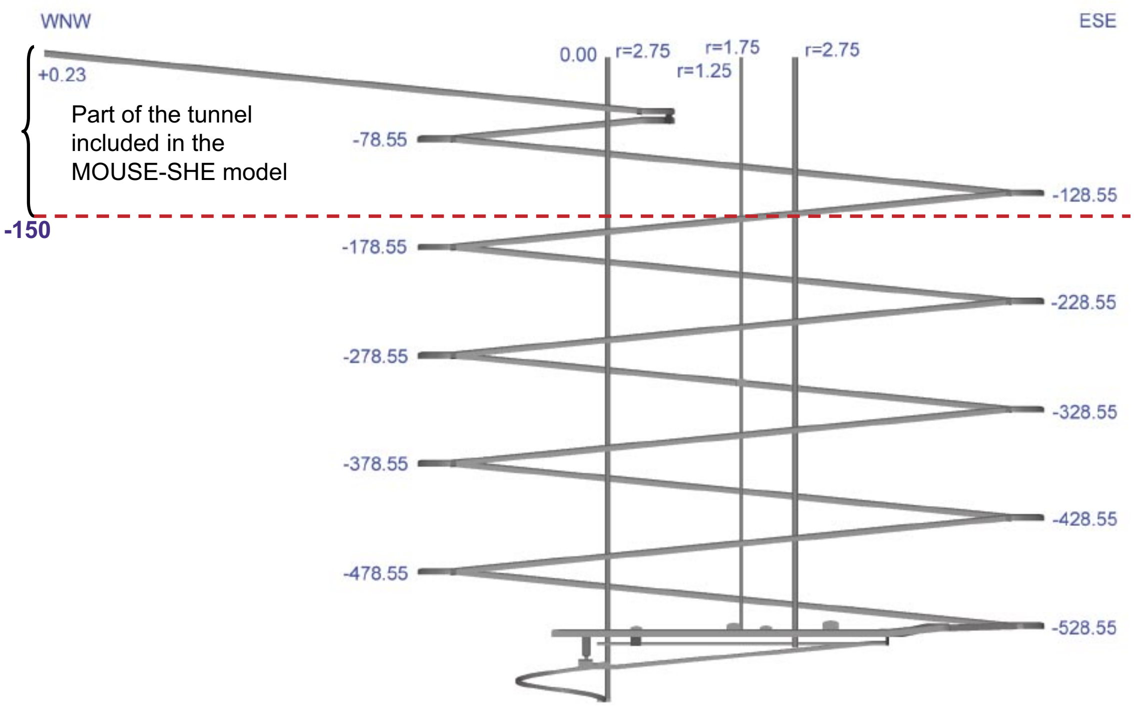

Figure 4-1. Layout of the tunnel and shaft.

4.2 Simulation cases

Three different cases have been defined according to different levels of grouting. The thickness of the grouted zone in the rock is set to 8 m which means that $LC_p = K_h/8$. The grouting levels are:

1. No grouting
2. $K = 1 \cdot 10^{-7} \rightarrow LC_p = 1.25 \cdot 10^{-8}$, $[s^{-1}]$
3. $K = 1 \cdot 10^{-9} \rightarrow LC_p = 1.25 \cdot 10^{-10}$, $[s^{-1}]$

Beside the three grouting cases, a sensitivity analysis was performed. The sensitivity analysis aimed at investigating the influence of the properties of the upper bedrock and the properties in the interface between the bedrock and the Quaternary deposits. The sensitivity analysis was only performed for the grouting case, $K = 1 \cdot 10^{-9}$.

The work flow is illustrated in Figure 4-2. All the simulation cases are described in Table 4-1. The base case model, BC, refers to the undisturbed model described in Chapter 3 and the different sensitivity cases, SA, refers to cases with alternative geological models. The numbers 1–3 in the name of the simulation cases denote the level of grouting and the letters a and b denote which bottom boundary condition that is used.

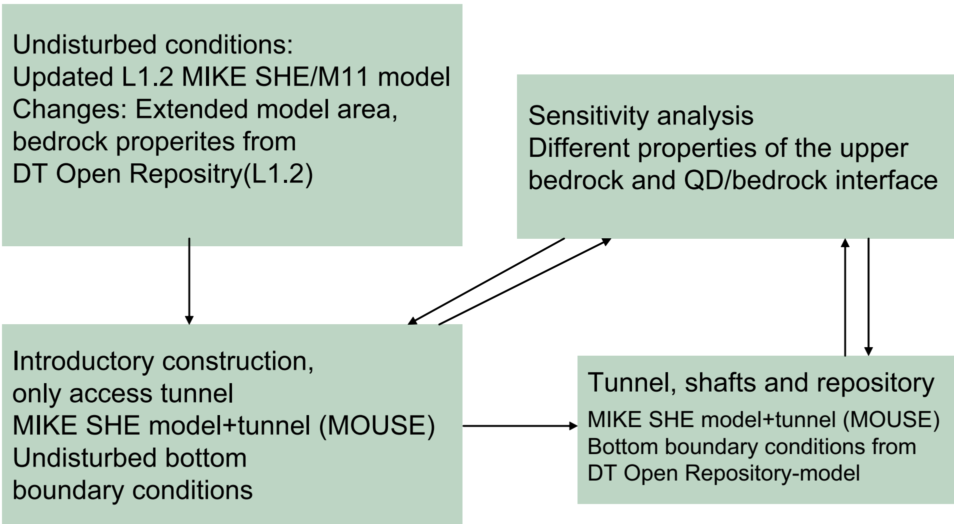

Figure 4-2. *Work flow for the open repository simulations.*

Table 4-1. Description of the simulation cases for the open repository calculations.

Simulation case	[1]Shaft and ramp	[2]Repository	Grouting	Bedrock model
BC_1a	X		No grouting	from DarcyTools
BC_2a	X		1.00E–07	from DarcyTools
BC_3a	X		1.00E–09	from DarcyTools
BC_1b	X	X	No grouting	from DarcyTools
BC_2b	X	X	1.00E–07	from DarcyTools
BC_3b	X	X	1.00E–09	from DarcyTools
SA_1a	X		1.00E–09	Homogenous bedrock, K = 1E–7, from –45 m up to QD model
SA_1b	X	X	1.00E–09	Homogenous bedrock, K = 1E–7, from –45 m up to QD model
SA_2a	X		1.00E–09	Homogenous bedrock, K = 1E–7, from –45 m up to QD model + a low permeable layer in the QD/bedrock interface. K_low = 1E–8
SA_2b	X	X	1.00E–09	Homogenous bedrock, K = 1E–7, from –45 m up to QD model + a low permeable layer in the QD/bedrock interface. K_low = 1E–8
SA_3a	X		1.00E–09	From Darcy Tools + a low permeable layer in the QD/bedrock interface. K_low = 1E–7
SA_3b	X	X	1.00E–09	From Darcy Tools + a low permeable layer in the QD/bedrock interface. K_low = 1E–7
SA_4a	X		1.00E–09	From Darcy Tools + a low permeable layer in the QD/bedrock interface. K_low = 1E–8
SA_4b	X	X	1.00E–09	From Darcy Tools + a low permeable layer in the QD/bedrock interface. K_low = 1E–8

1. Undisturbed bottom boundary condition from DarcyTools.
2. Bottom boundary conditions from a DarcyTools simulation where the repository was included.

4.3 Presentation of open repository results

The calculations have been made for two different bottom boundary conditions. The first case had the same bottom boundary condition as the calculations for the undisturbed conditions. I.e. the calculated head at 150 m below sea level. from DarcyTools (under undisturbed conditions) was imported to the MIKE SHE model, except for the area near the tunnel construction and the shafts. In this area, a no-flow boundary was applied in the model. Had a fixed head in a calculation cell intersected by a water pipe in MOUSE been used, the fixed head will generate an unrealistic inflow of water to the tunnel. This case aimed to describe the introductory construction, the period when only the access tunnel and shafts has been built. In the second case the calculated head from the DarcyTools Open repository /Svensson 2006/ simulations were imported to the MIKE SHE model. The Darcy Tools model has the whole repository and the shafts up the ground surface implemented in the model. Different boundary conditions have been implemented depending on the level of grouting. When the lowest level of grouting, $K_g = 1 \cdot 10^{-7}$ m/s, is applied the boundary condition is taken from the corresponding grouting case in DarcyTools.

The results are presented in two parts. The first part presents the results from the base case simulations, case BC_1–BC_3. In these calculations, the basis for the modelling is the model described in Chapter 3, i.e. the bedrock model is the "original model" from DarcyTools and the model for the QD is the same as in the L1.2 MIKE SHE model. The second part presents the results from the sensitivity analysis, case SA_1–SA_4. In case BC_1–BC_3 the whole repository is open at the same time. A special case, BC_4, has also been studied. In this case only part A and C are open, Figure 4-3.

For all the BC-cases where the repository is included, the boundary condition is taken from the corresponding case in DarcyTools. This means that if the level of grouting corresponds to a K-value of the tunnel wall of $1 \cdot 10^{-9}$ m/s, the boundary condition from Darcy Tools is taken from a simulation with this level of grouting. For case SA_1b–4b the boundary condition is taken from the Darcy Tools case where the level of grouting was set to 1E–9 m/s. The cases with the homogenous bedrock and the low permeable layer in the QD/bedrock interface have not been studied in DarcyTools.

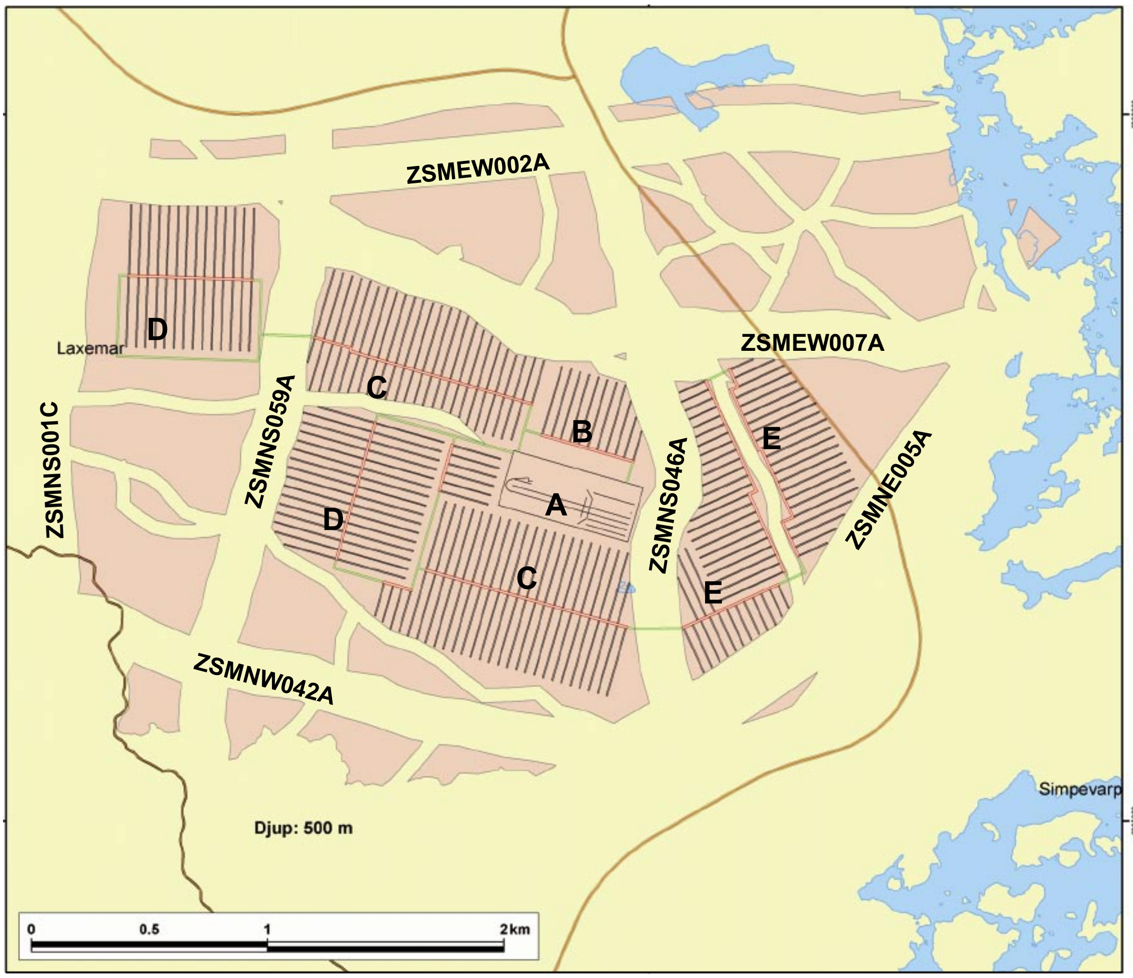

__Figure 4-3__. Different parts of the repository. In case SA_1b–SA_3b all parts are open. In case SA_4 only part A and C are open.

4.4 Results of base case simulations

4.4.1 Water balance

The inflow of water to the tunnel and shafts during the introductory construction is very small compared to the total turnover of water in the area; thus, the water balance in the area is not strongly affected of the introductory construction of the tunnel and shafts. On the other hand, when the repository is included in the modelling, the run-off from the area and the total evapotranspiration are reduced. Due to numerical instabilities the results from case BC_1b, when no grouting is applied and the repository is included in the modelling, are not presented in this report.

The total evapotranspiration is reduced from 474 mm during undisturbed conditions to 452 mm when the repository is implemented and the highest level of grouting is applied to the tunnel walls, case BC_3b. Figure 4-4 presents the run-off from the area for cases BC1– BC4. For case BC_1a–3a the runoff is not affected. When the repository is included, case BC1b–3b, the run-off is reduced between 40% and 20% compared to undisturbed conditions depending on the level of grouting and how much of the repository that is open at the same time, Figure 4-4. When the lowest level of grouting is applied and the whole repository is open at the same time, BC_2b, the run-off from the water courses is reduced by 44%. When the higher level of grouting is applied and only parts A and C are open, case BC_4, the run-off is reduced by 20%. The reduction of the water transported to M11 is in the same range both from the over land compartment and from the saturated zone.

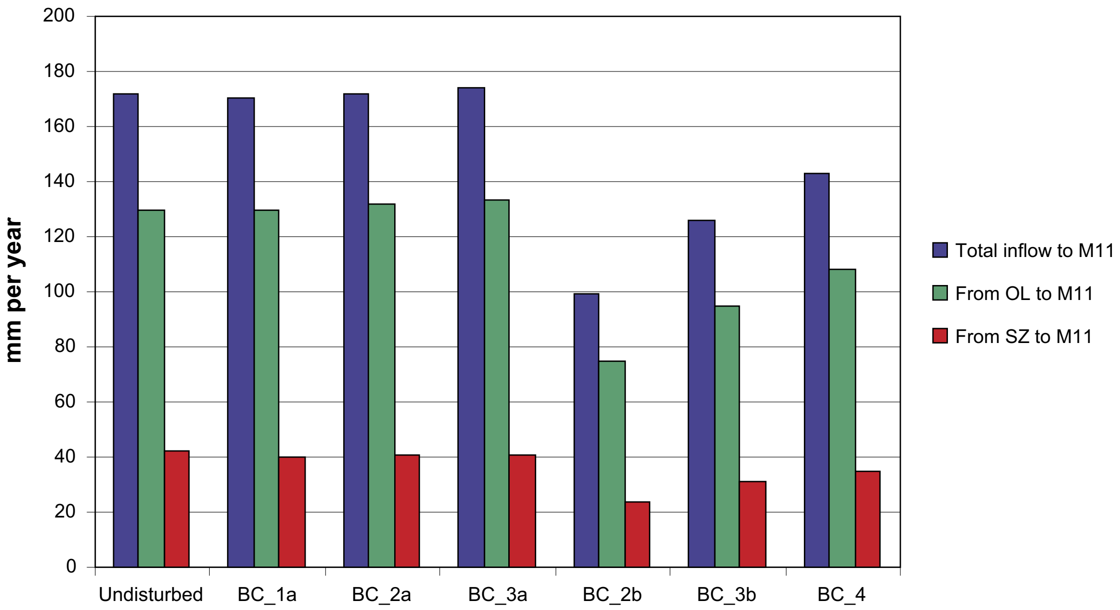

Figure 4-4*. Run-off from the water courses in the model area for all BC-cases.*

4.4.2 Inflow to tunnel and shafts

The inflows to the tunnel and shafts are in the same range for all the BC-cases. When no grouting is applied the total inflow is calculated to 5.6 l/s and when the highest level of grouting is applied the inflow is calculated to 4.6 l/s. The inflows for case BC_1a–3a are listed in Table 4-2 . The inflows are highest in the beginning of the simulated year. The inflows decrease during the simulation and are almost stabilised after one year, Figure 4-5.

When introducing the repository, the inflows to the tunnel construction in the MOUSE-SHE model are still in the same range as for the undisturbed bottom boundary condition. Since the MOUSE-SHE model describes the uppermost 150 m of the tunnel, the inflows are independent of the bottom boundary condition representing the repository. However, when introducing the repository the flow over the bottom boundary is increased. The sum of the inflows to the tunnel and shafts and the flow over the bottom boundary can be seen as the potential total inflow to the repository. This sum can be compared to the calculated inflows to the repository from DarcyTools and it gives an estimation of the two models accordance. The results show a better agreement between the models for the cases where the highest level of grouting is applied, K = 1E–9 m/s. In this case the calculated inflow to the repository from DarcyTools is to 33 l/s and the sum of the inflows to the tunnels and the flow over the bottom boundary in MIKE SHE is 43 l/s. When only part A and C is open the agreement is even better, 19 l/s calculated with DarcyTools compared to 17 l/s calculated with MOUSE-SHE. The results are presented in Figure 4-6.

The inflow to the tunnel is dependent on the properties of the surrounding bedrock; thus, the inflows are varying along the tunnel. The meteorological conditions are also reflected in the calculated inflows. The inflows are higher during intensive periods of rain. Figure 4-7 shows the water flow in the tunnel at different depths below ground surface during the simulated year.

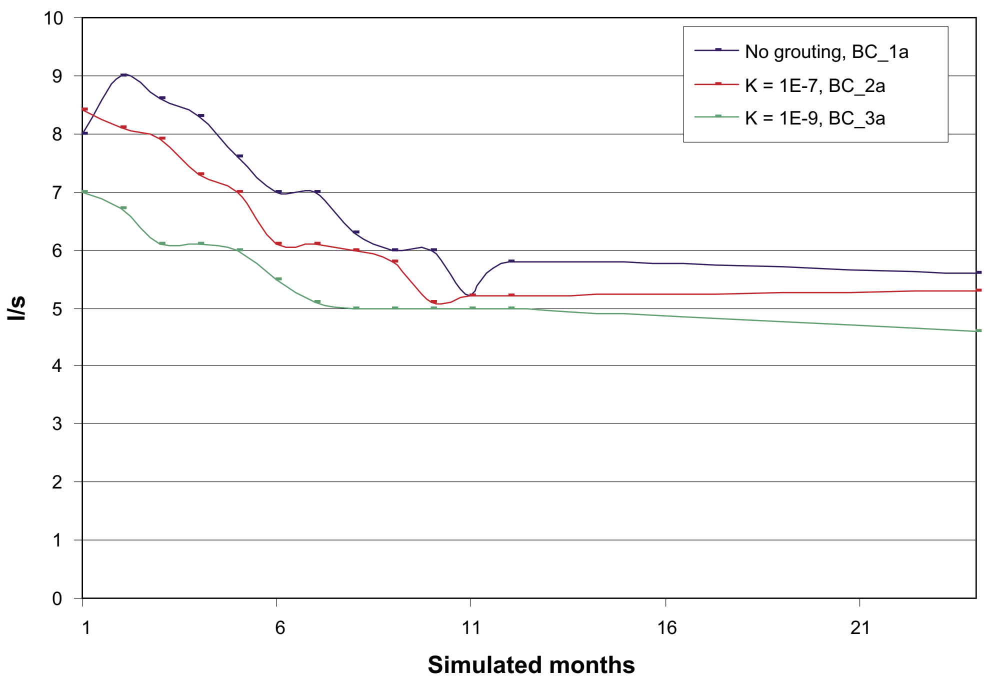

***Figure 4-5.** Inflow to the tunnel versus time. The inflow is reduced during the simulation and is almost stable after one year of simulation.*

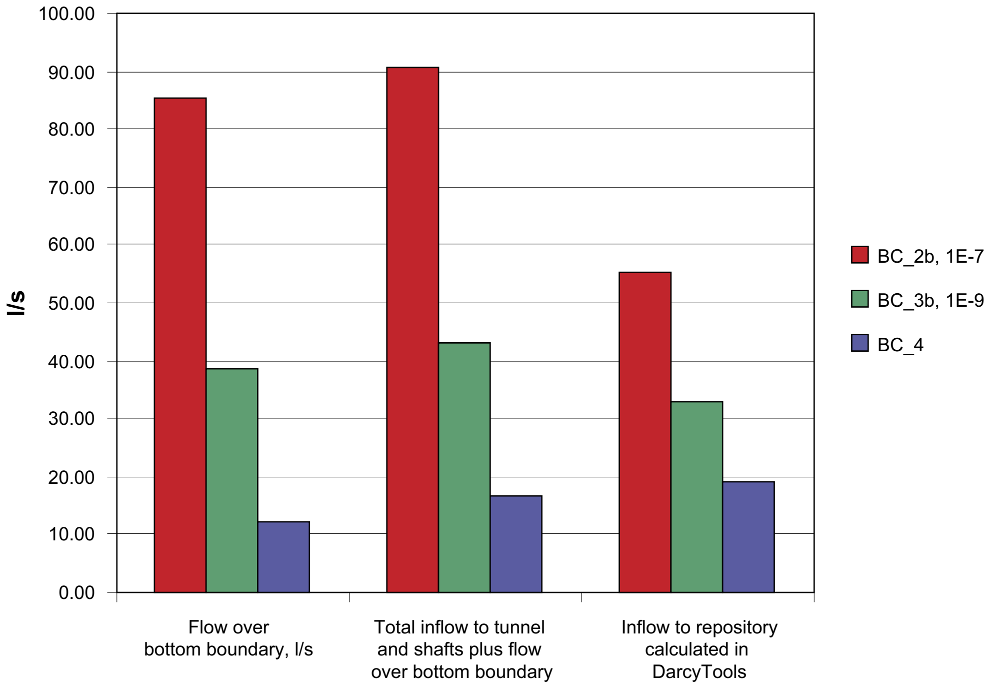

***Figure 4-6**. Flow over bottom boundary plus inflow to tunnel and shafts compared to calculated inflow to the repository.*

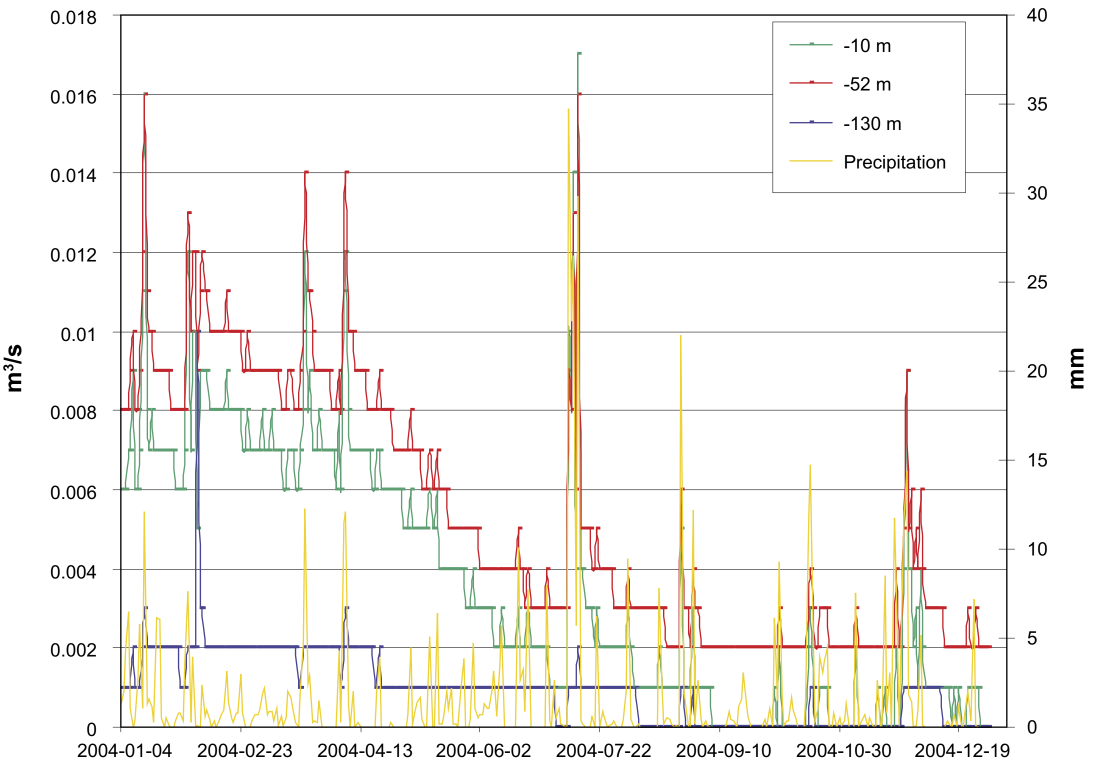

***Figure 4-7.** Inflow to the tunnel at different depths below ground during the simulated year.*

Table 4-2. Calculated inflows to the tunnel and shafts for case BC_1a–3a, i.e. for the introductory construction without the deep parts of the repository.

	Total inflow to the tunnel, l/s (yearly mean)
BC_1a (No grouting, bedrock model from DarcyTools)	5.6
BC_2a (K_g = 1E–7, bedrock model from DarcyTools)	5.3
BC_3a (K_g = 1E–9, bedrock model from DarcyTools)	4.6

4.4.3 Surface water levels and discharges in water courses

The only lake in the modelled area is Lake Frisksjön. The mean depth of Lake Frisksjön is not affected by the repository and tunnel constructions. The low permeable clay layer under the lake in the model has a strong influence on the lake level and prevents a lowering of the water level in the lake.

The total area with ponded water (saturated areas) is not noticeably affected by the introductory construction. When the repository is introduced in the model the total saturated area is decreased. The saturated areas in the model area decrease with 10% when the lower level of grouting is applied and with 5% when the higher level of grouting is applied, Figure 4-8.

The discharges in the water courses are not affected by the introductory construction of the tunnel and shafts. The discharge is affected when the repository is introduced in the model. The influence is local. The water course in the catchment area that is underlain by the largest part of the repository is also the water course where the strongest decreasing of the discharge is observed. Under undisturbed conditions the specific discharge in catchment area number 9, Ekerumsbäcken, is calculated to 6.3 l/s km^2. When the lowest level of grouting is applied to the repository and tunnel walls the specific discharge decreases to 1.5 l/s km^2, the water course will be dry during most of the year. When the highest level of grouting is applied the specific discharge is calculated to 2.6 l/s km^2. A hydrograph from the outlet of the water course is shown in Figure 4-9.

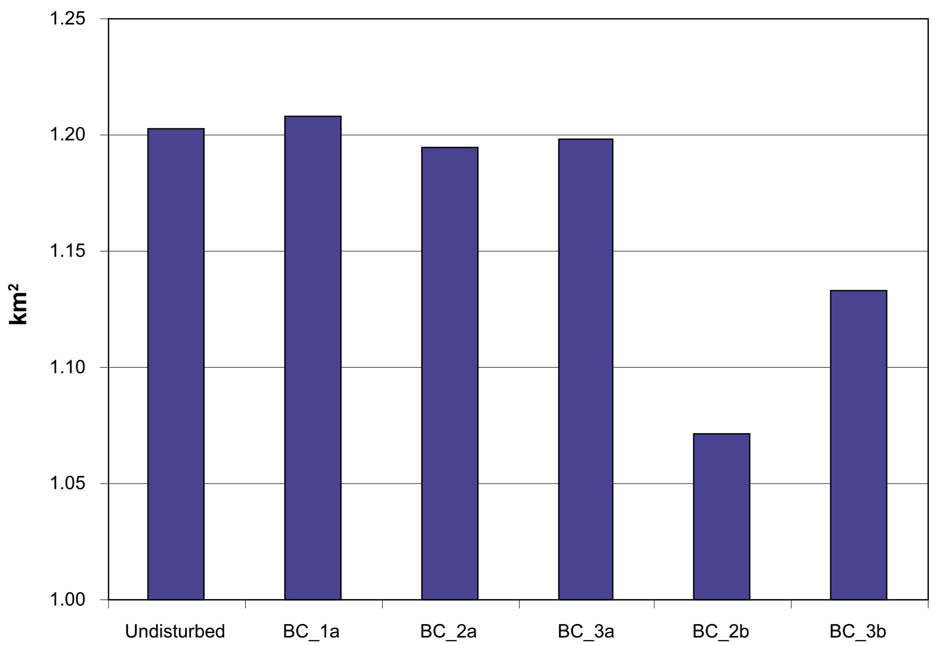

***Figure 4-8**. Total area with ponded water for the different BC-cases.*

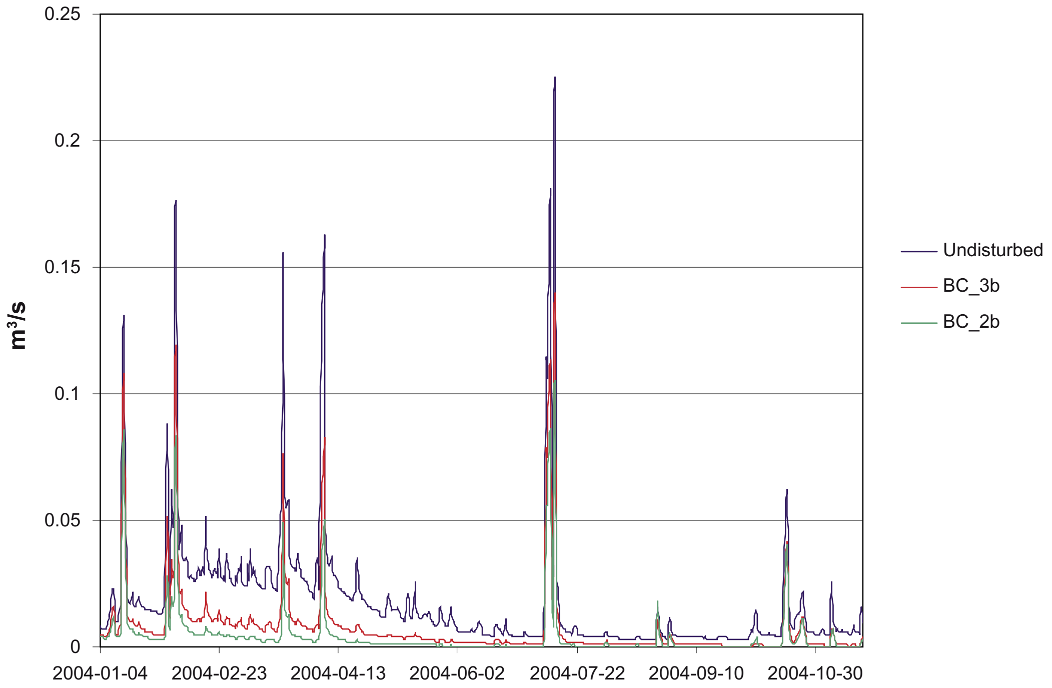

Figure 4-9. *Discharge in Ekerumsbäcken, catchment area number 9, for undisturbed conditions, BC_2b (Bedrock model from DT and K_g = 1E–7) and BC_3b (Bedrock model from DT and K_g = 1E–9).*

4.4.4 Groundwater levels and head drawdown

The influence area, which here is defined as the area where the groundwater table has been lowered more than 0.3 m, is highly dependent on the level of grouting. The maximum lowering of the ground water table occurs in the case where no grouting is applied (Figure 4-10 and Table 4-3). During the introductory construction when no grouting is applied, case BC_1a, the groundwater level drops to the bottom of the model, 150 m below sea level, and the influence area is calculated to 1.6 km^2. In case BC_3a, where the highest level of grouting is applied, the influence area is calculated to 1.17 km^2, a decrease with approximately 30%. When the highest level of grouting is applied, case BC_3a, there is no visible lowering of the water table around the shaft in the NW part of the model area, Figure 4-11. Without grouting, a lowering of the water table around the shaft with about ten metres has been calculated, Figure 4-10.

Table 4-3. Influence area for case BC_1a–3a, the lowering of the water table during the introductory construction.

Case	Maximum lowering of the water table, m	Influence area, km^2	Area where the lowering of the water table is > 1 m	Area where the lowering of the water table is > 5 m	Area where the lowering of the water table is > 10 m	Area where the lowering of the water table is > 20 m
BC_1a, No grouting	150	1.59	1.007	0.423	0.204	0.099
BC_2a, K_g = 1E–7	83	1.38	0.871	0.383	0.178	0.08
BC_3a, K_g = 1E–9	66	1.17	0.704	0.248	0.096	0.026

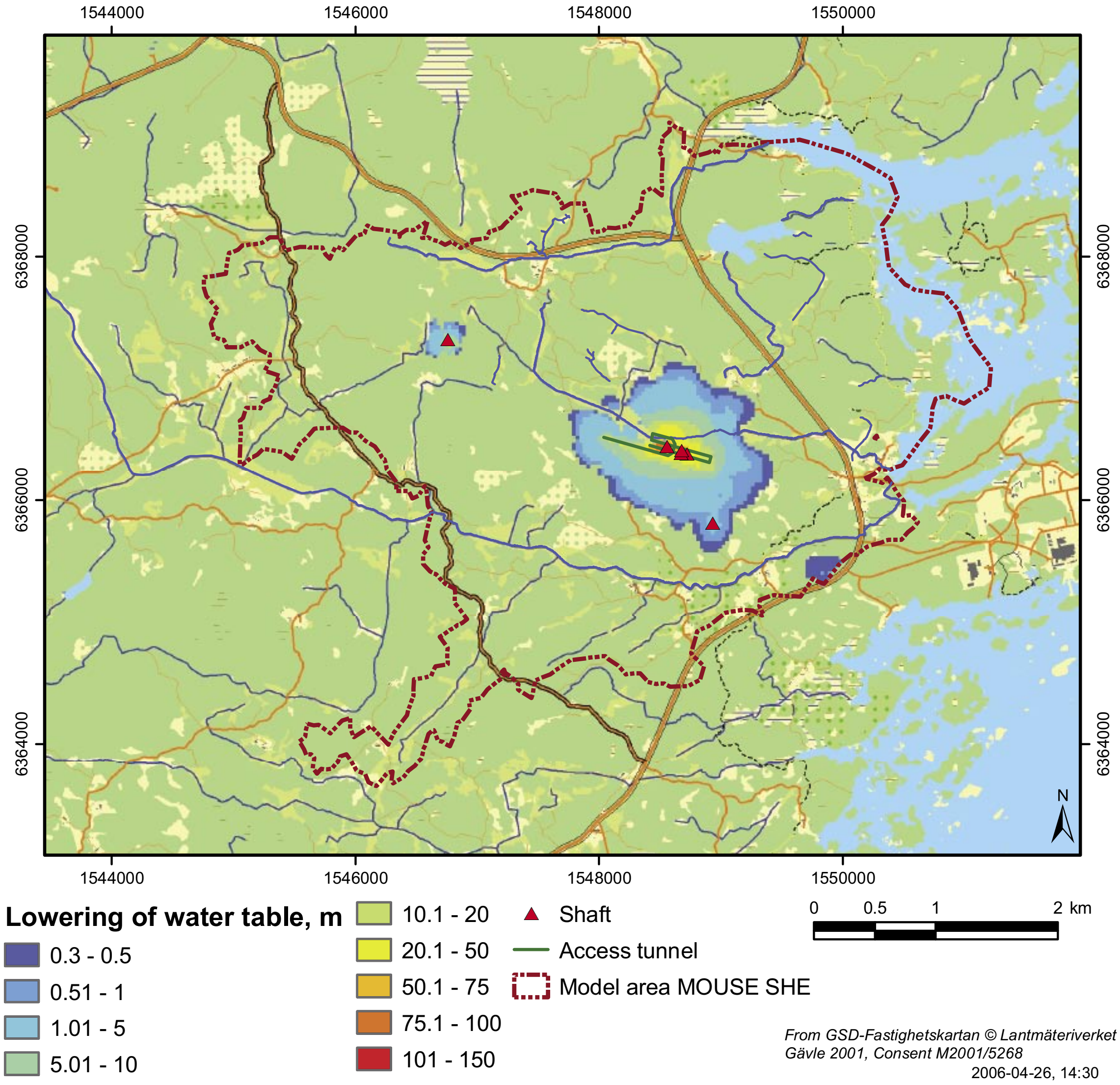

Figure 4-10. *Lowering of the groundwater table, Case BC_1a, in the case where no grouting is applied. The access tunnel and the shafts are marked in the figure.*

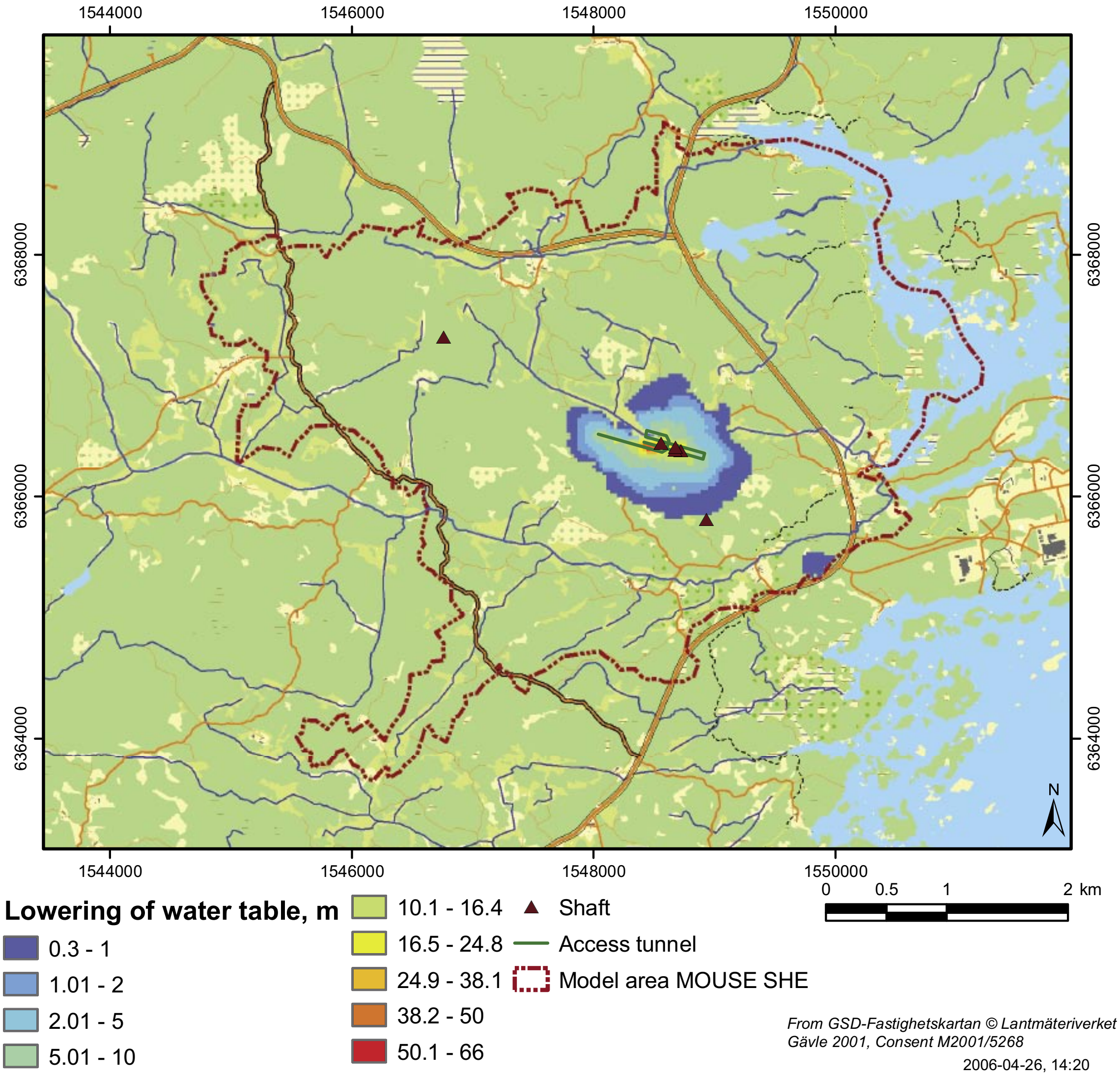

***Figure 4-11.** Lowering of the groundwater table, Case BC_3a, the access tunnel and the shafts are marked in the figure.*

The introduction of the deep parts of the repository in the model has a strong influence on the lowering of the water table. In case BC_3b, when the highest level of grouting is applied to the repository and the tunnel walls, the influence area is calculated to 9 km^2. The groundwater table drops most close to the access tunnel and the central part of the repository, cf Figure 4-12. An area of 4.3 km^2 is lowered more than 5 m and an area of only 1.8 km^2 is lowered more than 20 m, see Table 4-4.

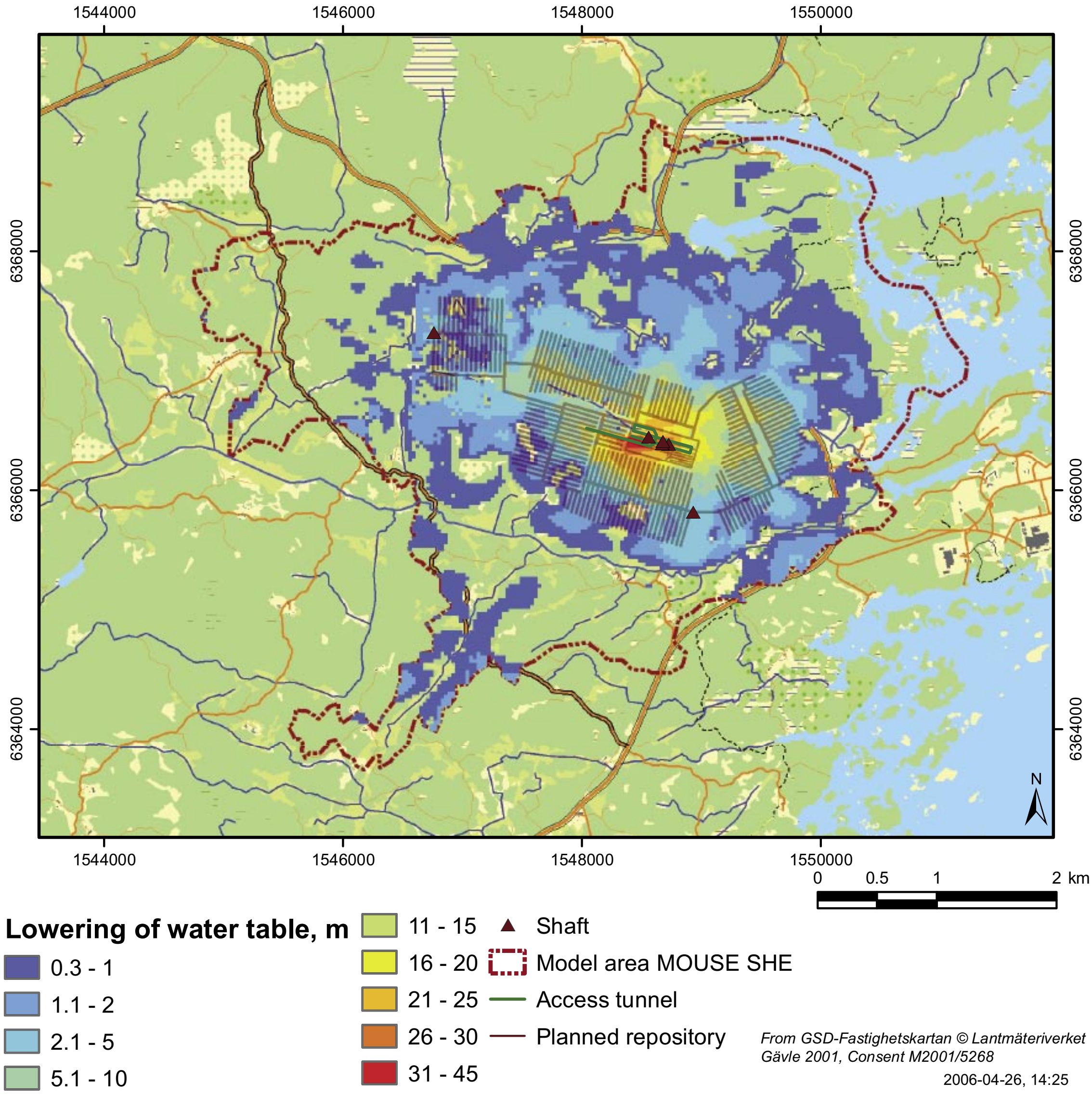

Figure 4-12. *Lowering of the water table in case BC_3b, i.e. the highest level of grouting is applied. The planned repository and the shafts are marked in the figure.*

Table 4-4. Influence area for case BC_2b, BC_3b and BC_4.

Case	Influence area, km²	Area where the lowering of the water table is > 1 m	Area where the lowering of the water table is > 5 m	Area where the lowering of the water table is > 10 m	Area where the lowering of the water table is > 20 m
BC_2b, K_g = 1E–7	11.28	8.23	4.32	3.13	1.84
BC_3b, K_g = 1E–9	9.18	5.36	1.73	0.84	0.203
BC_4, Part A and C open	7.38	3.02	0.53	0.21	0.02

A vertical profile of the model showing the calculation layers, the head in each calculation layer and the ground water table is illustrated in Figure 4-13. The blue marks indicate where the tunnel intersects the cross section. The groundwater table, the thick blue line in Figure 4-13, drops down to a level of 60 m below sea level. The head, in a calculation layer, can never be lower than the lower level of the calculation layer; that is why the head in the

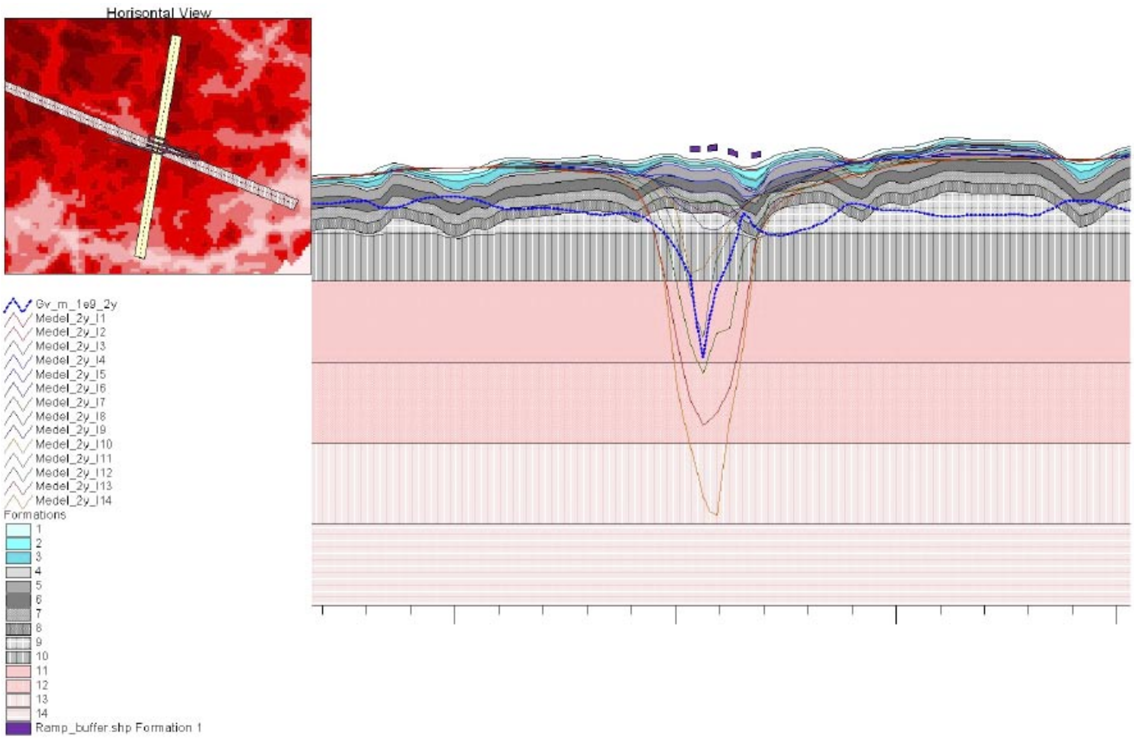

Figure 4-13. *Vertical profile showing the calculation layers, the head in each calculation layer and the groundwater table. The blue marks at the ground surface indicates where the tunnel intersects the cross section.*

upper calculation layers are above the groundwater table in the figure. In the lower calculation layers, the head drawdown is larger than the lowering of the water table. The figure illustrates the head drawdown for case BC_3b, i.e. the repository is included and the highest level of grouting is applied. It is seen in the figure that the cone of depression is located close to the access tunnel. The access tunnel has a strong influence on the drawdown, the lowering of the water table is much lower outside the central area of the repository.

4.5 Results from sensitivity analysis

A sensitivity analysis of the open repository calculations was performed. The analysis aims at investigating the sensitivity of the model to the properties of the upper bedrock and the properties of the QD/bedrock interface. The different cases are described in Table 4-1, Section 4.2. Two main parts can be identified in the different cases. In case SA_1ab–SA_2ab the upper bedrock, from 45 m below sea level, is homogenous with a K-value of $1 \cdot 10^{-7}$ m/s. In case SA_3ab–SA_4ab the "original bedrock model" from DarcyTools is used, but a 1.5 m thick low permeable layer is introduced in the QD/bedrock interface.

The results show that the most sensitive part of the model results are the lowering of the water table. The influence area is highly dependent on the properties in the QD/bedrock interface; a low permeable layer in the interface has a noticeable effect on the lowering of the water table. The inflows to the tunnel and shafts are not sensitive to the properties of the upper bedrock or the properties of the QD/bedrock interface.

4.5.1 Lowering of the water table

The model is more sensitive to the properties in the QD/bedrock interface than to the considered variations in the properties of the upper bedrock, Figure 4-14. In case SA_1a, where the upper bedrock is assumed to be homogenous with a K-value = $1 \cdot 10^{-7}$ m/s, the influence area increases with a few percent compared to the reference case, BC_3a. When a low permeable layer is assumed in the QD/bedrock interface above the homogenous bedrock, case SA_2a, the influence area is a few percent smaller than for the reference case. The assumed homogenous upper bedrock is more permeable than the "original" bedrock model, which leads to a larger influence area.

When the low permeable layer is implemented above the homogenous bedrock, the influence area becomes a little smaller than for the reference case. The low permeable layer acts as a barrier. The largest difference from the reference case is noticed for case SA_3a and SA_4a. In these cases the original bedrock model is used, but a low permeable layer is introduced between the bedrock and the QD-model. In case SA_4a the K-value of the low permeable layer is set to $1 \cdot 10^{-8}$ m/s, which gives the smallest influence area and the lowest maximum lowering of the water table. The influence area decreases with 66% compared to case BC_3a when a low permeable layer, $K = 1 \cdot 10^{-8}$ m/s, is assumed between the QD-model and the bedrock. The maximum lowering of the water table and the influence area for all sensitivity cases describing the introductory construction is listed in Table 4-5.

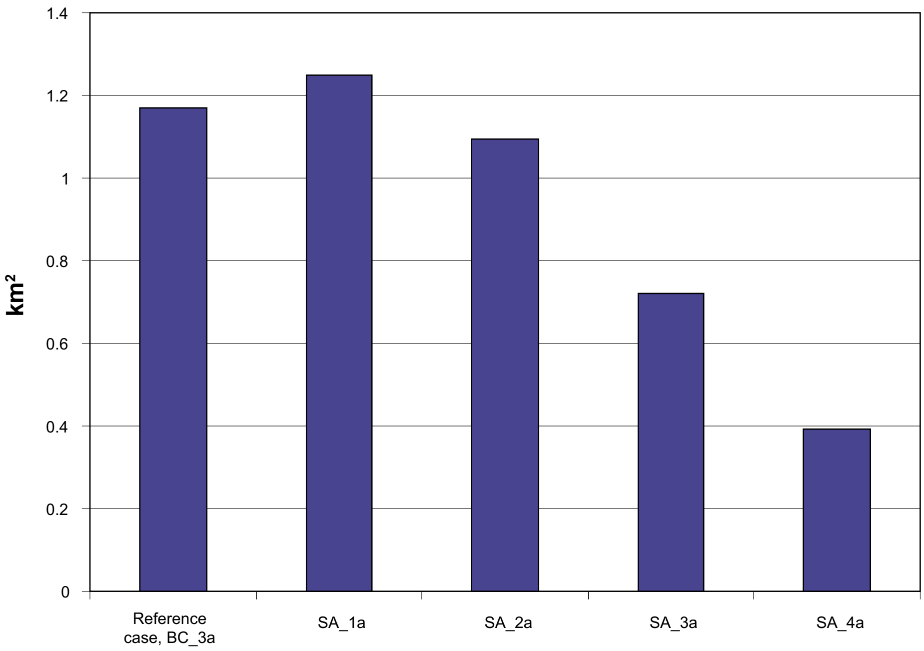

Figure 4-14. *Influence area for case SA1a–SA4a. The reference case, BC_3a where the highest level of grouting is applied to the tunnel walls and the "original" bedrock model is used is also shown in the figure.*

Table 4-5. Influence area for case SA_1a–4a, the lowering of the water table during the introductory construction.

	Maximum lowering of the water table, m	Influence area, km^2	Area where the lowering of the water table is > 1 m	Area where the lowering of the water table is > 5 m	Area where the lowering of the water table is > 10 m	Area where the lowering of the water table is > 20 m
BC_3a, Reference case	66	1.17	0.704	0.248	0.096	0.026
SA_1a (Homogenous bedrock up to –45 m below sea level, $K_{bedrock}$ = 1E–7)	77	1.248	0.761	0.356	0.206	0.071
SA_2a (Homogenous bedrock up to –45 m below sea level, $K_{bedrock}$ = 1E–7 + low permeable layer in QD/bedrock interface)	45	1.095	0.428	0.217	0.085	0.017
SA_3a (Bedrock model from DT + low permeable layer in QD/bedrock interface, K = 1E–7)	60	0.719	0.515	0.185	0.066	0.017
SA_4a (Bedrock model from DT + low permeable layer in QD/bedrock interface, K = 1E–8)	30	0.394	0.225	0.034	0.013	0.003

The low permeable layer has the same effect when the repository is introduced in the model. There is an evident decrease of the influence area in case SA_3b and SA_4b. The low permeable layer, which is only 1.5 m thick, has a large influence on the lowering of the water table. The influence area decreases from 9.18 km^2 to 3.10 km^2 in case SA_4b, a reduction with almost 70%. The influence area is larger for case SA_1b than for the reference case; the homogenous upper bedrock causes a larger lowering of the water table than the "original" bedrock model. The low permeable layer has a larger effect in case SA_2b than in case SA_2a, the influence area is smaller compared to the reference case when the repository is included in the modelling. The influence areas for all sensitivity cases where the repository is included in the model are listed in Table 4-6 and illustrated in Figure 4-15.

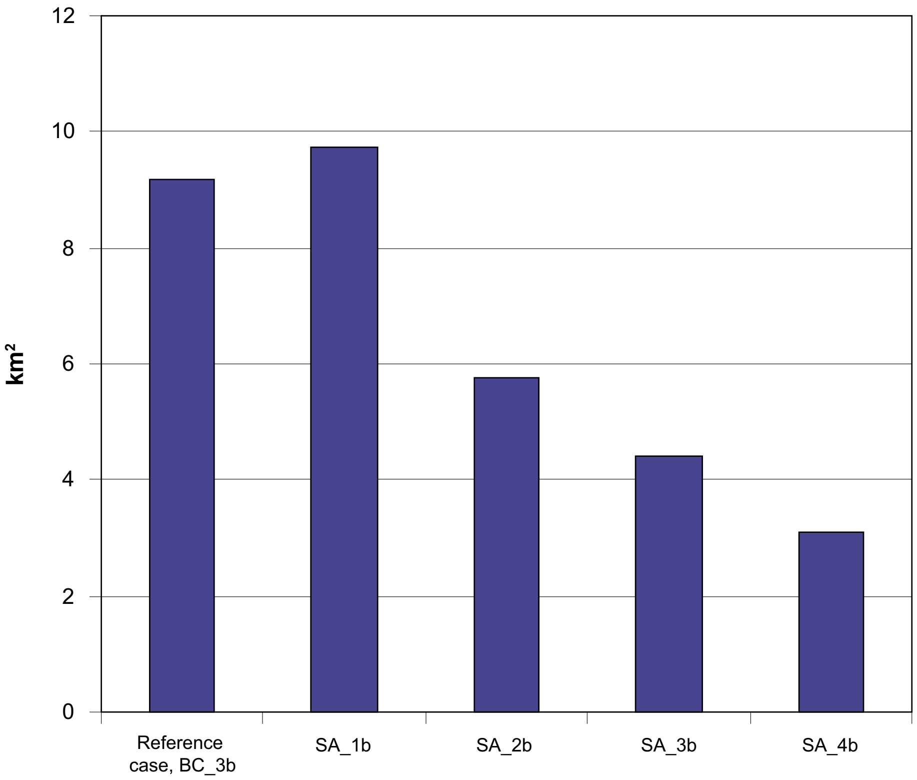

Figure 4-15. *Influence area for case SA_1b–4b.*

Table 4-6. Influence area for case SA_1b–4b, the cases where the repository is implemented in the model.

	Influence area, km²	Area where the lowering of the water table is > 1 m	Area where the lowering of the water table is > 5 m	Area where the lowering of the water table is > 10 m	Area where the lowering of the water table is > 20 m
Reference case, BC_3b	9.18	5.36	1.73	0.84	0.203
SA_1b (Homogenous bedrock up to –45 m below sea level, $K_{bedrock}$ = 1E–7)	9.740	6.737	2.458	1.414	0.329
SA_2b (Homogenous bedrock up to –45 m below sea level, $K_{bedrock}$ = 1E–7 + low permeable layer in QD/bedrock interface)	5.756	3.022	1.094	0.368	0.034
SA_3b (Bedrock model from DT + low permeable layer in QD/bedrock interface, K = 1E–7)	4.420	2.859	1.213	0.532	0.095
SA_4b (Bedrock model from DT + low permeable layer in QD/bedrock interface, K = 1E–8)	3.098	2.022	0.590	0.227	0.019

4.5.2 Inflows to tunnel and shafts

The inflows to tunnel and shafts are not that sensitive to the upper bedrock properties or the properties in the QD/bedrock interface. The inflows to the tunnel and shafts are in the range 4–6 l/s for all sensitivity cases describing the introductory construction, Figure 4-16.

4.5.3 Run-off in the water courses

The run-off to MIKE 11 is reduced in all sensitivity cases compared to the run-off under undisturbed conditions, Figure 4-17. The run-off varies between 120 and 140 mm. The lowest run-off is calculated in case SA_1b. This result agrees with the results for the lowering of the water table. The largest lowering of the water table was calculated for this case. It is noticed that a large drawdown causes a lower run-off from the area.

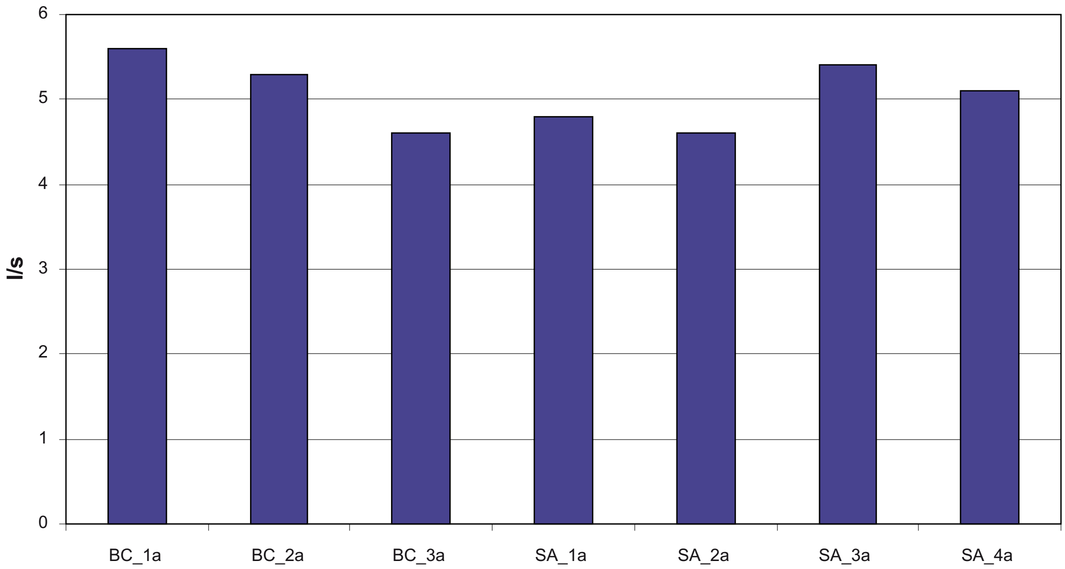

Figure 4-16*. Inflows to tunnel and shafts for all sensitivity cases.*

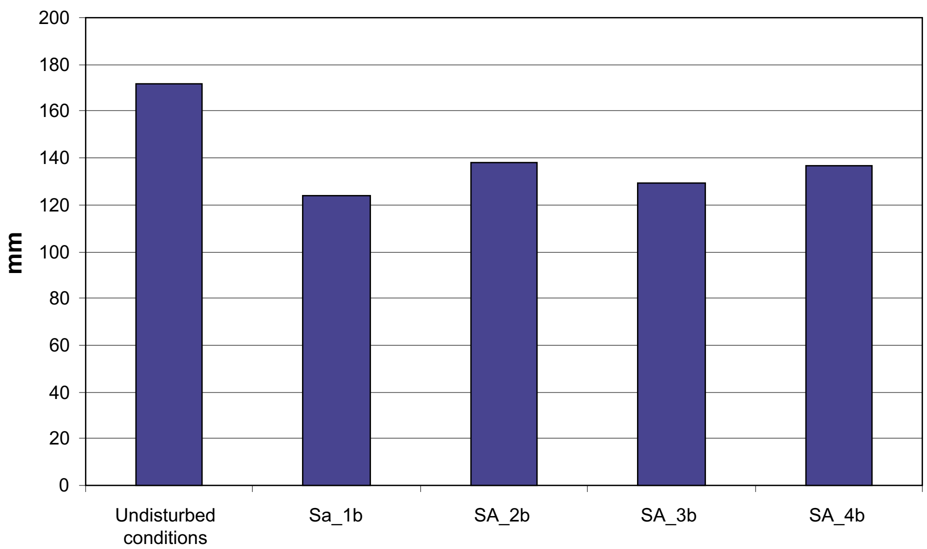

Figure 4-17*. Water transport from MIKE SHE to M11 for case SA_1b–SA_4b.*

5 Summary and conclusions

5.1 Summary of results for undisturbed conditions

The results presented in Chapter 3 agrees with the results from the L1.2 MIKE SHE model /Werner et al. 2005b/. The water balance is in the same range in the two models. The total run-off from the model is calculated to 188 mm. The run-off in the L1.2 MIKE SHE model was calculated to 189 mm. The calculated specific discharge from the water courses in the model is 5.5 $l/s \cdot km^2$. The discharge in the water courses is transient during the year. The groundwater table is shallow in the area, the mean depth to the groundwater table during the simulated year is 0.7 m.

5.2 Summary of the open repository results

The head drawdown and the size of the influence area are dependent on the level of grouting. "The worst case scenario" when no grouting is used, leads to an influence area of 1.6 km^2 during the introductory construction. When the repository is implemented, the repository walls have to be grouted to avoid numerical instabilities. No results have been presented for the case with no grouting when the repository in included in the modelling. When the highest level of grouting is applied to the repository walls, the influence area is calculated to 9.2 km^2. The large effects are however local and the largest lowering of the groundwater table is concentrated to the tunnel constructions. It is seen in Table 4-4 that the area that is lowered more than 20 m is very small compared to the total influence area (defined as the area where the groundwater table drops more than 0.3 m). Even if the groundwater level drops some ten metres locally, there are no visible effects on the surface water levels in the lake in the model area. The low permeable clay layer under the lake in the model acts as a barrier and prevents a lowering of the lake water level.

The inflows to the tunnel are in the same range for all levels of grouting. They vary between 4–6 l/s depending on the applied level of grouting. The inflows are not affected by the lower boundary condition which represents the deep parts of the repository in the cases where this is considered. The inflows in the upper 150 m of the access tunnel are still between 4–6 l/s when the repository is included in the calculations. There is an agreement between MIKE SHE and the DarcyTools model of the open repository. The calculated inflows to the repository in DarcyTools are in the same range as the sum of water leaving the model via MOUSE (i.e.the water that enters the upper part of the tunnel) and over the bottom boundary in MIKE SHE. The agreement is best for the cases where the highest level of grouting is applied to the tunnel walls. The inflows to the tunnel vary with depth and time. It is dependent on the weather condition and the properties of the surrounding bedrock. The inflow increases during periods of intense rains and at locations where the tunnel intersects relatively high conductive zones.

The discharges in the water courses in the area are not affected by the introductory construction of the access tunnel and shafts. When the whole repository is open the discharge is reduced by 20–40% depending on the level of grouting applied to the tunnel walls. The reduction of the discharge is local; the largest decrease was noticed in the catchment area containing the largest part of the repository.

The results are sensitive to the properties of the QD/bedrock interface. A low permeable layer, only 1.5 m thick, has large consequences for the size of the influence area and the magnitude of the lowering of the water table. A low permeable layer with a K-value = $1 \cdot 10^{-8}$ m/s reduces the influence area with almost 70%. The surface water levels are not affected by the repository. The only lake in the area, Lake Frisksjön, is in the model underlain by a 4 m thick layer of low permeable clay. This clay acts as a barrier and prevents a lowering of the lake water level. This result agrees with the results from the sensitivity analysis where the lowering of the water table is strongly reduced if a low permeable layer is assumed at the QD/bedrock interface.

Excavations and drillings performed at the site during 2006 indicates thick layers of Quaternary deposits in some of the valleys in Laxemar. The valleys are often underlain by larger fracture zones /Sohlenius et al. 2006/. In the QD-model used as input data to the MIKE SHE model, a mean depth of the clay is set to c 3–4 m depending of the clay type (post glacial or glacial clay). The clay is underlain by 3.6 m of till, which results in a total depth of c 7 m in areas covered by clay. The results from the latest investigations indicate a larger depth of QD, in some areas the QD-depth is more than 30 m. In the sensitivity analysis a 1.5 m thick, low permeable layer was implemented all over the whole model area. This is unrealistic but it is, however, a way to investigate how low permeable clay layers can reduce the effects of an open repository. It is probable that the same results would have been reached if the low permeable layer only was implemented in areas underlain by fracture zones, these areas are areas which are in contact with the repository depth and causes the largest drawdown. The latest investigations /Sohlenius et al. 2006/ point out that the valleys in the Laxemar area are covered by thicker layers of clay and till than used in this modelling. Complementary investigations, which aim to investigate the properties of the QD/Bedrock interface and the total QD-depth in some valleys in the Laxemar area, will be performed during the autumn 2006.

5.3 Evaluation of uncertainties

The present MIKE SHE simulations of the Laxemar area are based on limited site data on the geological and hydrogeological properties of the modelled system. Specifically, a simplified stratigraphic model of the Quaternary deposits is used, and the available hydraulic dataset does not include site-specific parameters for all materials represented in the flow model.

It follows that there are a number of uncertainties associated with the application of the simulation results for describing the present surface hydrological and near-surface hydrogeological conditions within the Laxemar area and the effects of an open repository. The main uncertainties can be summarised as follows:

- Uncertainties in input data and models from other disciplines:
  - The topographical description (the DEM).
  - The geological descriptions of bedrock and Quaternary deposits (spatial distribution and stratigraphy).
  - The vegetation map.
- Uncertainties in the classification and parametrisation of different types of vegetation for use in the modelling of evapotranspiration and unsaturated flow.
- Uncertainties in the hydraulic parameters for saturated flow in Quaternary deposits and fractured rock. Especially the properties of the upper bedrock and the zone between the Quaternary deposits and the bedrock. There are also uncertainties related to the parameters for unsaturated flow.

- Uncertainties related to simplifications in process models in MIKE SHE, primarily in the modelling of unsaturated flow and soil freezing/thawing.
- Uncertainties related to the implementation of the tunnel and shafts.

Generally, the uncertainties associated with the limited application of site data in the flow modelling are judged most important at the present stage of model development. The reasons for these uncertainties are related both to the limited availability of site data and to limitations in the analyses performed. The present data gaps concern both basic properties of the system (e.g. hydrogeological parameters on some QD) and data needed to evaluate the model (e.g. measured flow rates). The MIKE SHE model describing undisturbed conditions are not calibrated against site data. In the time of modelling there were not long enough time series available to perform a calibration.

The vegetation classification is based on field inventory of the tree layer. The classification and the parameters describing the properties of each vegetation class are associated with uncertainties; these parameters affect the water balance through the modelling of the evapotranspiration. Since the potential evapotranspiration is the maximum evapotranspiration, the different parameters have a moderate effect on the actual evapotranspiration. It is only the K_c-value (defined as actual transpiration/potential evaporation) that can make the actual transpiration larger than the potential evapotranspiration.

The description of the surface water system is important for the modelling of surface hydrology and near-surface hydrogeology. In particular, the various threshold levels and flow resistances in the water courses determine, together with the hydrogeological properties, the distribution of the total run-off on the surface and subsurface systems. There has been a field inventory of the cross sections of the water courses and the slope of the river bed in almost all water courses included in the model. For water courses that have not been investigated in the field, the cross sections in the MIKE 11 river network are assumed to have triangular shapes and the depth from the bank level to the bottom is set to 1 m.

The description of the tunnel and the shafts has to be further analysed. There has not been time for a sensitivity study of the MOUSE-SHE coupling in this project.

The MOUSE-SHE simulations have only been run for three years, two years of introductory construction and one year with an open repository. The effects of the tunnel and the repository are evident and the ground water level in the area is strongly affected by the tunnel construction and the bottom boundary condition mimicking the repository. It is possible that the effects of the tunnel and shafts would be larger if the model was run for a longer period, i.e. it is possible that the system has not reached a "semi steady-state condition".

5.4 Conclusions

The effects on the hydrology and near-surface hydrogeology are evident during the period when the repository is air-filled. The head drawdown in the bedrock causes a lowering of the water table and the discharge in the water courses decreases. With the present model of the bedrock the repository has to be grouted to a relatively high level, $K_g = 1 \cdot 10^{-7}$, to avoid numerical instabilities caused by that the groundwater table drops to repository depth. Even when the highest level of grouting is applied the influence area (defined as the area where the groundwater table drops more than 0.3 m) is calculated to 9 km^2. However, the results are sensitive to the hydrogeological model for the bedrock and the description of the interface between the bedrock and the Quaternary deposits. A thin layer of clay reduces the lowering of the water table and the influence area considerable. Investigations performed during the autumn 2005 indicate large depth of QD and low permeable layers over the fracture zones, this information is not used in the present model. Complementary investigations during 2006 will further analyse the depth of QD and the hydraulic properties of the same. This will be very valuable information in coming versions of the MIKE SHE model.

6 References

Bosson E, Berglund S, 2005. Kontroll och inmätning av diken i potentiella utströmnings-områden i Laxemar. Valideringstest av ythydrologisk modellering. SKB P-05-238. Svensk Kärnbränslehantering AB.

Bosson E, Berglund S, 2006. Near-surface hydrogeological model of Forsmark. Open repository and solute transport applications – Forsmark 1.2. SKB R-06-52. Svensk Kärnbränslehantering AB.

Boresjö Bronge L, Wester K, 2003. Vegetation mapping with satellite data of the Forsmark, Tierp and Oskarshamn regions. SKB P-03-83. Svensk Kärnbränslehantering AB.

Brydsten L, Strömgren M, 2005. Digital elevation models for site investigation program in Oskarshamn. Site description version 1.2. SKB P-05-38. Svensk Kärnbränslehantering AB.

DHI Software, 2004a. MIKE SHE User's Guide.

DHI Software, 2004b. MOUSE User's Guide.

DHI Sverige, VBB VIAK, 1998. Dokumentation av MIKE SHE-modellen för Kristianstadsslätten.

Domenico P-A, Schwartz F W, 1998. Physical and chemical hydrogeology (2nd ed). John Wiley & Sons Inc, New York.

Gustafsson L-G, Vikström M, 2006. Modelling transport of water and solutes in future wetlands in Forsmark. SKB R-06-46. Svensk Kärnbränslehantering AB.

Johansson P-O, Werner K, Bosson E, Berglund S, Juston J, 2005. Description of climate, surface hydrology, and near-surface hydrogeology. Preliminary site description Forsmark – version 1.2. SKB R-05 -06. Svensk Kärnbränslehantering AB.

Johansson T, Adestam L, 2004b. Oskarshamn site investigation. Slug tests in groundwater monitoring wells in soil in the Simpevarp area. SKB P-04-122. Svensk Kärnbränslehantering AB.

Johansson T, Adestam L, 2004d. Slug tests in groundwater monitoring wells in soil in the Laxemar area. SKB P-04-318. Svensk Kärnbränslehantering AB.

Kellner E, 2003. Wetlands – different types, their properties and functions. SKB TR-04-08. Svensk Kärnbränslehantering AB.

Knutsson G, Morfeldt C-O, 2002. Grundvatten – teori och tillämpning. Svensk Byggtjänst AB (in Swedish).

Lindborg T (ed), 2006. Description of surface systems. Preliminary site description Laxemar subarea – version 1.2. SKB R-06-11. Svensk Kärnbränslehantering AB.

Nyman H, 2005. Depth and stratigraphy of Quaternary deposits in the Simpevarp area. An application of the GeoEditor modelling tool. SKB R-05-54. Svensk Kärnbränslehantering AB.

Rhén I (ed), Gustafson G, Stanfors R, Wikberg P, 1997. Äspö HRL – Geoscienteific evaluation 1997/5. Models based on site characterization 1986–1995. SKB TR-97-06. Svensk Kärnbränslehantering AB.

Rudmark L, 2004. Oskarshamn site investigation. Investigation of Quaternary deposits at Simpevarp peninsula and the islands of Ävrö and Hålö. SKB P-04-22. Svensk Kärnbränslehantering AB.

Rudmark L, Malmberg-Persson K, Mikko H, 2005. Oskarshamn site investigation – Investigation of Quaternary deposits 2003–2004. SKB P-05-49. Svensk Kärnbränslehantering AB.

SKB, 2005. Preliminary site description. Simpevarp subarea – version 1.2. SKB R-05-08. Svensk Kärnbränslehantering AB.

SKB, 2006. Preliminary site description. Laxemar subarea – version 1.2. SKB R-06-10. Svensk Kärnbränslehantering AB.

Sohlenius G, Bergman T, Snäll S, Lundin L, Lode E, Stendahl J, Riise A, Nilsson J, Johansson T, Göransson M, 2006. Oskarshamn site investigation, Soils, Quaternary deposits and bedrock in topographic lineaments situated in the Laxemar subarea. SKB P-06-XX. Svensk Kärnbränslehantering AB

Strömgren M, Brydsten L, Lindgren F, 2006. Oskarshamn site investigation. Measurements of Brook gradients. SKB P-06-05. Svensk Kärnbränslehantering AB.

Svensson U, 2006. The Laxemar repository – Modelling changes in the flow, pressure and salinity fields, due to a repository for spent nuclear fuel. SKB R-06-57. Svensk Kärnbränslehantering AB.

Werner K, Bosson E, Berglund S, 2005a. Description of climate, surface hydrology, and near-surface hydrogeology. Simpevarp 1.2. SKB R-05-04. Svensk Kärnbränslehantering AB.

Werner K, Bosson E, Berglund S, 2005b. Description of climate, surface hydrology, and near-surface hydrogeology. Preliminary site description Laxemar subarea – version 1.2. SKB R-05-61. Svensk Kärnbränslehantering AB.

Appendix 1

The total conductance of the walls of the shafts is varying with the level of grouting. The values used for each shaft in the different grouting cases are listed in Table A1-1 to A1-18. The calculation of the conductance is described in Section 2.1.2.

Table A1-1. Geometry and conductivity for shaft S1 when no grouting is applied to the walls of the shafts.

Calculation layer	Circumference, m	Kh, m/s	Dx	Thickness of calculation layer, m	Conductance, m²/s
1	9.42	2.36E–07	20	1	6.98E–07
2	9.42	2.36E–07	20	1	6.98E–07
3	9.42	2.36E–07	20	1	6.98E–07
4	9.42	2.36E–07	20	1	6.98E–07
5	9.42	2.36E–07	20	4	2.79E–06
6	9.42	2.36E–07	20	4	2.79E–06
7	9.42	2.36E–07	20	4	2.79E–06
8	9.42	2.36E–07	20	4	2.79E–06
9	9.42	2.05E–07	20	19.3	1.17E–05
10	9.42	1.14E–07	20	18	6.07E–06
11	9.42	1.25E–09	20	30	1.11E–07
12	9.42	2.84E–09	20	30	2.52E–07
13	9.42	7.78E–10	20	30	6.90E–08
14	9.42	7.19E–10	20	30	6.38E–08

Table A1-2. Geometry and conductivity for shaft S2 when no grouting is applied to the walls of the shafts.

Calculation layer	Circumference, m	Kh, m/s	Dx	Thickness of calculation layer, m	Conductance, m²/s
1	6.28	4.00E–05	20	1	7.89E–05
2	6.28	4.00E–05	20	1	7.89E–05
3	6.28	4.00E–05	20	2	1.58E–04
4	6.28	6.13E–06	20	1	1.21E–05
5	6.28	3.72E–06	20	4	2.93E–05
6	6.28	1.01E–06	20	4	7.97E–06
7	6.28	1.01E–06	20	4	7.97E–06
8	6.28	1.10E–07	20	4	8.68E–07
9	6.28	8.28E–08	20	4.1	6.69E–07
10	6.28	2.92E–08	20	18	1.04E–06
11	6.28	1.01E–10	20	30	5.97E–09
12	6.28	1.01E–10	20	30	5.97E–09
13	6.28	1.01E–10	20	30	5.97E–09
14	6.28	1.01E–10	20	30	5.97E–09

Table A1-3. Geometry and conductivity for shaft S3 when no grouting is applied to the walls of the shafts.

Calculation layer	Circumference, m	Kh, m/s	Dx	Thickness of calculation layer, m	Conductance, m²/s
1	17.27	1.38E–06	20	1	1.19163E–06
2	17.27	1.01E–06	20	1	8.72135E–07
3	17.27	1.01E–06	20	1	8.72135E–07
4	17.27	1.01E–06	20	1	8.72135E–07
5	17.27	1.01E–06	20	4	3.48854E–06
6	17.27	1.01E–06	20	4	3.48854E–06
7	17.27	1.01E–06	20	4	3.48854E–06
8	17.27	9.64E–07	20	4	3.32966E–06
9	17.27	1.50E–07	20	11.7	1.51544E–06
10	17.27	4.15E–08	20	18	6.45035E–07
11	17.27	1.30E–08	20	30	3.36765E–07
12	17.27	1.00E–07	20	30	2.5905E–06
13	17.27	5.31E–08	20	30	1.37556E–06
14	17.27	4.47E–09	20	30	1.15795E–07

Table A1-4. Geometry and conductivity for shaft S4 when no grouting is applied to the walls of the shafts.

Calculation layer	Circumference, m	Kh, m/s	Dx	Thickness of calculation layer, m	Conductance, m²/s
1	7.85	8.86E–06	20	1.7	5.91184E–06
2	7.85	1.30E–05	20	1	5.1025E–06
3	7.85	1.01E–06	20	1	3.96425E–07
4	7.85	1.01E–06	20	1	3.96425E–07
5	7.85	1.01E–06	20	4	1.5857E–06
6	7.85	1.01E–06	20	4	1.5857E–06
7	7.85	1.01E–06	20	4	1.5857E–06
8	7.85	7.38E–07	20	4	1.15866E–06
9	7.85	1.15E–07	20	11.5	5.19081E–07
10	7.85	3.10E–08	20	18	2.19015E–07
11	7.85	7.97E–10	20	30	9.38468E–09
12	7.85	2.14E–08	20	30	2.51985E–07
13	7.85	5.52E–08	20	30	6.4998E–07
14	7.85	4.04E–08	20	30	4.7571E–07

Table A1-5. Geometry and conductivity for shaft S5 when no grouting is applied to the walls of the shafts.

Calculation layer	Circumference, m	Kh, m/s	Dx	Thickness of calculation layer, m	Conductance, m²/s
1	10.99	1.06E–06	20	1	3.66E–06
2	10.99	1.01E–06	20	1	3.49E–06
3	10.99	1.01E–06	20	1	3.49E–06
4	10.99	1.01E–06	20	1	3.49E–06
5	10.99	1.01E–06	20	4	1.39E–05
6	10.99	1.01E–06	20	4	1.39E–05
7	10.99	1.01E–06	20	4	1.39E–05
8	10.99	1.01E–06	20	4	1.39E–05
9	10.99	1.05E–07	20	13.1	4.75E–06
10	10.99	1.92E–09	20	18	1.19E–07
11	10.99	2.18E–09	20	30	2.26E–07
12	10.99	2.30E–07	20	30	2.38E–05
13	10.99	2.89E–07	20	30	2.99E–05
14	10.99	2.48E–07	20	30	2.57E–05

Table A1-6. Geometry and conductivity for shaft S6 when no grouting is applied to the walls of the shafts.

Calculation layer	Circumference, m	Kh, m/s	Dx	Thickness of calculation layer, m	Conductance, m²/s
1	17.27	3.00E–05	20	1	1.63E–04
2	17.27	3.81E–05	20	1	2.07E–04
3	17.27	4.00E–05	20	3.8	8.24E–04
4	17.27	3.00E–06	20	1	1.63E–05
5	17.27	1.11E–06	20	4	2.41E–05
6	17.27	1.01E–06	20	4	2.19E–05
7	17.27	5.76E–06	20	4	1.25E–04
8	17.27	4.28E–08	20	4	9.28E–07
9	17.27	4.28E–08	20	2.2	5.11E–07
10	17.27	9.20E–08	20	18	8.98E–06
11	17.27	6.48E–08	20	30	1.05E–05
12	17.27	6.10E–08	20	30	9.92E–06
13	17.27	1.07E–07	20	30	1.74E–05
14	17.27	1.07E–07	20	30	1.74E–05

Table A1-7. Geometry and conductivity for shaft S1 when the grouting K = 1E–7 is applied to the walls of the shafts.

Calculation layer	Circum-ference, m	Kh, m/s	Dx, m	Thickness of calulation layer, m	Lc_aq, s^{-1}	LC_shaft, s^{-1}	Lc_tot, s^{-1}	Conductance, m^2/s
1	9.42	2.36E–07	20	1	1.18E–08	1.25E–08	6.07E–09	5.72E–08
2	9.42	2.36E–07	20	1	1.18E–08	1.25E–08	6.07E–09	5.72E–08
3	9.42	2.36E–07	20	1	1.18E–08	1.25E–08	6.07E–09	5.72E–08
4	9.42	2.36E–07	20	1	1.18E–08	1.25E–08	6.07E–09	5.72E–08
5	9.42	2.36E–07	20	4	1.18E–08	1.25E–08	6.07E–09	2.29E–07
6	9.42	2.36E–07	20	4	1.18E–08	1.25E–08	6.07E–09	2.29E–07
7	9.42	2.36E–07	20	4	1.18E–08	1.25E–08	6.07E–09	2.29E–07
8	9.42	2.36E–07	20	4	1.18E–08	1.25E–08	6.07E–09	2.29E–07
9	9.42	2.05E–07	20	19.3	1.03E–08	1.25E–08	5.63E–09	1.02E–06
10	9.42	1.14E–07	20	18	5.70E–09	1.25E–08	3.91E–09	6.64E–07
11	9.42	1.25E–09	20	30	6.25E–11	1.25E–08	6.22E–11	1.76E–08
12	9.42	2.84E–09	20	30	1.42E–10	1.25E–08	1.40E–10	3.97E–08
13	9.42	7.78E–10	20	30	3.89E–11	1.25E–08	3.88E–11	1.10E–08
14	9.42	7.19E–10	20	30	3.60E–11	1.25E–08	3.58E–11	1.01E–08

Table A1-8. Geometry and conductivity for shaft S2 when the grouting K = 1E–7 is applied to the walls of the shafts.

Calculation layer	Circum-ference, m	Kh, m/s	Dx, m	Thickness of calulation layer, m	Lc_aq, s^{-1}	LC_shaft, s^{-1}	Lc_tot, s^{-1}	Conductance, m^2/s
1	6.28	4.00E–05	20	1	2.00E–06	1.25E–08	1.24E–08	7.80E–08
2	6.28	4.00E–05	20	1	2.00E–06	1.25E–08	1.24E–08	7.80E–08
3	6.28	4.00E–05	20	2	2.00E–06	1.25E–08	1.24E–08	1.56E–07
4	6.28	6.13E–06	20	1	3.07E–07	1.25E–08	1.20E–08	7.54E–08
5	6.28	3.72E–06	20	4	1.86E–07	1.25E–08	1.17E–08	2.94E–07
6	6.28	1.01E–06	20	4	5.05E–08	1.25E–08	1.00E–08	2.52E–07
7	6.28	1.01E–06	20	4	5.05E–08	1.25E–08	1.00E–08	2.52E–07
8	6.28	1.10E–07	20	4	5.50E–09	1.25E–08	3.82E–09	9.59E–08
9	6.28	8.28E–08	20	4.1	4.14E–09	1.25E–08	3.11E–09	8.01E–08
10	6.28	2.92E–08	20	18	1.46E–09	1.25E–08	1.31E–09	1.48E–07
11	6.28	1.01E–10	20	30	5.05E–12	1.25E–08	5.05E–12	9.51E–10
12	6.28	1.01E–10	20	30	5.05E–12	1.25E–08	5.05E–12	9.51E–10
13	6.28	1.01E–10	20	30	5.05E–12	1.25E–08	5.05E–12	9.51E–10
14	6.28	1.01E–10	20	30	5.05E–12	1.25E–08	5.05E–12	9.51E–10

Table A1-9. Geometry and conductivity for shaft S3 when the grouting K = 1E–7 is applied to the walls of the shafts.

Calculation layer	Circum-ference, m	Kh, m/s	Dx, m	Thickness of calulation layer, m	Lc_aq, s^{-1}	LC_shaft, s^{-1}	Lc_tot, s^{-1}	Conductance, m^2/s
1	17.27	1.38E–06	20	1	6.90E–08	1.25E–08	1.06E–08	1.83E–07
2	17.27	1.01E–06	20	1	5.05E–08	1.25E–08	1.00E–08	1.73E–07
3	17.27	1.01E–06	20	1	5.05E–08	1.25E–08	1.00E–08	1.73E–07
4	17.27	1.01E–06	20	1	5.05E–08	1.25E–08	1.00E–08	1.73E–07
5	17.27	1.01E–06	20	4	5.05E–08	1.25E–08	1.00E–08	6.92E–07
6	17.27	1.01E–06	20	4	5.05E–08	1.25E–08	1.00E–08	6.92E–07
7	17.27	1.01E–06	20	4	5.05E–08	1.25E–08	1.00E–08	6.92E–07
8	17.27	9.64E–07	20	4	4.82E–08	1.25E–08	9.93E–09	6.86E–07
9	17.27	1.50E–07	20	11.7	7.50E–09	1.25E–08	4.69E–09	9.47E–07
10	17.27	4.15E–08	20	18	2.08E–09	1.25E–08	1.78E–09	5.53E–07
11	17.27	1.30E–08	20	30	6.50E–10	1.25E–08	6.18E–10	3.20E–07
12	17.27	1.00E–07	20	30	5.00E–09	1.25E–08	3.57E–09	1.85E–06
13	17.27	5.31E–08	20	30	2.66E–09	1.25E–08	2.19E–09	1.13E–06
14	17.27	4.47E–09	20	30	2.24E–10	1.25E–08	2.20E–10	1.14E–07

Table A1-10. Geometry and conductivity for shaft S4 when the grouting K = 1E–7 is applied to the walls of the shafts.

Calculation layer	Circum-ference, m	Kh, m/s	Dx, m	Thickness of calulation layer, m	Lc_aq, s^{-1}	LC_shaft, s^{-1}	Lc_tot, s^{-1}	Conductance, m^2/s
1	7.85	8.86E–06	20	1.7	4.43E–07	1.25E–08	1.22E–08	1.62E–07
2	7.85	1.30E–05	20	1	6.50E–07	1.25E–08	1.23E–08	9.63E–08
3	7.85	1.01E–06	20	1	5.05E–08	1.25E–08	1.00E–08	7.87E–08
4	7.85	1.01E–06	20	1	5.05E–08	1.25E–08	1.00E–08	7.87E–08
5	7.85	1.01E–06	20	4	5.05E–08	1.25E–08	1.00E–08	3.15E–07
6	7.85	1.01E–06	20	4	5.05E–08	1.25E–08	1.00E–08	3.15E–07
7	7.85	1.01E–06	20	4	5.05E–08	1.25E–08	1.00E–08	3.15E–07
8	7.85	7.38E–07	20	4	3.69E–08	1.25E–08	9.34E–09	2.93E–07
9	7.85	1.15E–07	20	11.5	5.75E–09	1.25E–08	3.94E–09	3.56E–07
10	7.85	3.10E–08	20	18	1.55E–09	1.25E–08	1.38E–09	1.95E–07
11	7.85	7.97E–10	20	30	3.99E–11	1.25E–08	3.97E–11	9.35E–09
12	7.85	2.14E–08	20	30	1.07E–09	1.25E–08	9.86E–10	2.32E–07
13	7.85	5.52E–08	20	30	2.76E–09	1.25E–08	2.26E–09	5.32E–07
14	7.85	4.04E–08	20	30	2.02E–09	1.25E–08	1.74E–09	4.10E–07

Table A1-11. Geometry and conductivity for shaft S5 when the grouting K = 1E–7 is applied to the walls of the shafts.

Calculation layer	Circum-ference, m	Kh, m/s	Dx, m	Thickness of calulation layer, m	Lc_aq, s^{-1}	LC_shaft, s^{-1}	Lc_tot, s^{-1}	Conductance, m^2/s
1	10.99	1.06E–06	20	1	5.30E–08	1.25E–08	1.01E–08	1.11E–07
2	10.99	1.01E–06	20	1	5.05E–08	1.25E–08	1.00E–08	1.10E–07
3	10.99	1.01E–06	20	1	5.05E–08	1.25E–08	1.00E–08	1.10E–07
4	10.99	1.01E–06	20	1	5.05E–08	1.25E–08	1.00E–08	1.10E–07
5	10.99	1.01E–06	20	4	5.05E–08	1.25E–08	1.00E–08	4.40E–07
6	10.99	1.01E–06	20	4	5.05E–08	1.25E–08	1.00E–08	4.40E–07
7	10.99	1.01E–06	20	4	5.05E–08	1.25E–08	1.00E–08	4.40E–07
8	10.99	1.01E–06	20	4	5.05E–08	1.25E–08	1.00E–08	4.40E–07
9	10.99	1.05E–07	20	13.1	5.25E–09	1.25E–08	3.70E–09	5.32E–07
10	10.99	1.92E–09	20	18	9.60E–11	1.25E–08	9.53E–11	1.88E–08
11	10.99	2.18E–09	20	30	1.09E–10	1.25E–08	1.08E–10	3.56E–08
12	10.99	2.30E–07	20	30	1.15E–08	1.25E–08	5.99E–09	1.97E–06
13	10.99	2.89E–07	20	30	1.45E–08	1.25E–08	6.70E–09	2.21E–06
14	10.99	2.48E–07	20	30	1.24E–08	1.25E–08	6.22E–09	2.05E–06

Table A1-12. Geometry and conductivity for shaft S6 when the grouting K = 1E–7 is applied to the walls of the shafts.

Calculation layer	Circum-ference, m	Kh, m/s	Dx, m	Thickness of calulation layer, m	Lc_aq, s^{-1}	LC_shaft, s^{-1}	Lc_tot, s^{-1}	Conductance, m^2/s
1	17.27	3.00E–05	20	1	1.50E–06	1.25E–08	1.24E–08	2.14E–07
2	17.27	3.81E–05	20	1	1.91E–06	1.25E–08	1.24E–08	2.14E–07
3	17.27	4.00E–05	20	3.8	2.00E–06	1.25E–08	1.24E–08	8.15E–07
4	17.27	3.00E–06	20	1	1.50E–07	1.25E–08	1.15E–08	1.99E–07
5	17.27	1.11E–06	20	4	5.55E–08	1.25E–08	1.02E–08	7.05E–07
6	17.27	1.01E–06	20	4	5.05E–08	1.25E–08	1.00E–08	6.92E–07
7	17.27	5.76E–06	20	4	2.88E–07	1.25E–08	1.20E–08	8.28E–07
8	17.27	4.28E–08	20	4	2.14E–09	1.25E–08	1.83E–09	1.26E–07
9	17.27	4.28E–08	20	2.2	2.14E–09	1.25E–08	1.83E–09	6.94E–08
10	17.27	9.20E–08	20	18	4.60E–09	1.25E–08	3.36E–09	1.05E–06
11	17.27	6.48E–08	20	30	3.24E–09	1.25E–08	2.57E–09	1.33E–06
12	17.27	6.10E–08	20	30	3.05E–09	1.25E–08	2.45E–09	1.27E–06
13	17.27	1.07E–07	20	30	5.35E–09	1.25E–08	3.75E–09	1.94E–06
14	17.27	1.07E–07	20	30	5.35E–09	1.25E–08	3.75E–09	1.94E–06

Table A1-13. Geometry and conductivity for shaft S1 when the grouting K = 1E–9 is applied to the walls of the shafts.

Calculation layer	Circumference, m	Kh, m/s	Dx, m	Thickness of calulation layer, m	Lc_aq, s^{-1}	LC_shaft, s^{-1}	Lc_tot, s^{-1}	Conductance, m^2/s
1	9.42	2.36E–07	20	1	1.18E–08	1.25E–10	1.24E–10	1.17E–09
2	9.42	2.36E–07	20	1	1.18E–08	1.25E–10	1.24E–10	1.17E–09
3	9.42	2.36E–07	20	1	1.18E–08	1.25E–10	1.24E–10	1.17E–09
4	9.42	2.36E–07	20	1	1.18E–08	1.25E–10	1.24E–10	1.17E–09
5	9.42	2.36E–07	20	4	1.18E–08	1.25E–10	1.24E–10	4.66E–09
6	9.42	2.36E–07	20	4	1.18E–08	1.25E–10	1.24E–10	4.66E–09
7	9.42	2.36E–07	20	4	1.18E–08	1.25E–10	1.24E–10	4.66E–09
8	9.42	2.36E–07	20	4	1.18E–08	1.25E–10	1.24E–10	4.66E–09
9	9.42	2.05E–07	20	19.3	1.025E–08	1.25E–10	1.23E–10	2.25E–08
10	9.42	1.14E–07	20	18	5.7E–09	1.25E–10	1.22E–10	2.07E–08
11	9.42	1.25E–09	20	30	6.25E–11	1.25E–10	4.17E–11	1.18E–08
12	9.42	2.84E–09	20	30	1.42E–10	1.25E–10	6.65E–11	1.88E–08
13	9.42	7.78E–10	20	30	3.89E–11	1.25E–10	2.97E–11	8.38E–09
14	9.42	7.19E–10	20	30	3.595E–11	1.25E–10	2.79E–11	7.89E–09

Table A1-14. Geometry and conductivity for shaft S2 when the grouting K = 1E–9 is applied to the walls of the shafts.

Calculation layer	Circumference, m	Kh, m/s	Dx, m	Thickness of calulation layer, m	Lc_aq, s^{-1}	LC_shaft, s^{-1}	Lc_tot, s^{-1}	Conductance, m^2/s
1	6.28	4.00E–05	20	1	0.000002	1.25E–10	1.25E–10	7.85E–10
2	6.28	4.00E–05	20	1	0.000002	1.25E–10	1.25E–10	7.85E–10
3	6.28	4.00E–05	20	2	0.000002	1.25E–10	1.25E–10	1.57E–09
4	6.28	6.13E–06	20	1	3.065E–07	1.25E–10	1.25E–10	7.85E–10
5	6.28	3.72E–06	20	4	0.000000186	1.25E–10	1.25E–10	3.14E–09
6	6.28	1.01E–06	20	4	5.05E–08	1.25E–10	1.25E–10	3.13E–09
7	6.28	1.01E–06	20	4	5.05E–08	1.25E–10	1.25E–10	3.13E–09
8	6.28	1.10E–07	20	4	5.5E–09	1.25E–10	1.22E–10	3.07E–09
9	6.28	8.28E–08	20	4.1	4.14E–09	1.25E–10	1.21E–10	3.12E–09
10	6.28	2.92E–08	20	18	1.46E–09	1.25E–10	1.15E–10	1.30E–08
11	6.28	1.01E–10	20	30	5.05E–12	1.25E–10	4.85E–12	9.14E–10
12	6.28	1.01E–10	20	30	5.05E–12	1.25E–10	4.85E–12	9.14E–10
13	6.28	1.01E–10	20	30	5.05E–12	1.25E–10	4.85E–12	9.14E–10
14	6.28	1.01E–10	20	30	5.05E–12	1.25E–10	4.85E–12	9.14E–10

Table A1-15. Geometry and conductivity for shaft S3 when the grouting K = 1E–9 is applied to the walls of the shafts.

Calculation layer	Circumference, m	Kh, m/s	Dx, m	Thickness of calulation layer, m	Lc_aq, s^{-1}	LC_shaft, s^{-1}	Lc_tot, s^{-1}	Conductance, m^2/s
1	17.27	1.38E–06	20	1	6.90E–08	1.25E–10	1.25E–10	2.15E–09
2	17.27	1.01E–06	20	1	5.05E–08	1.25E–10	1.25E–10	2.15E–09
3	17.27	1.01E–06	20	1	5.05E–08	1.25E–10	1.25E–10	2.15E–09
4	17.27	1.01E–06	20	1	5.05E–08	1.25E–10	1.25E–10	2.15E–09
5	17.27	1.01E–06	20	4	5.05E–08	1.25E–10	1.25E–10	8.61E–09
6	17.27	1.01E–06	20	4	5.05E–08	1.25E–10	1.25E–10	8.61E–09
7	17.27	1.01E–06	20	4	5.05E–08	1.25E–10	1.25E–10	8.61E–09
8	17.27	9.64E–07	20	4	4.82E–08	1.25E–10	1.25E–10	8.61E–09
9	17.27	1.50E–07	20	11.7	7.50E–09	1.25E–10	1.23E–10	2.48E–08
10	17.27	4.15E–08	20	18	2.08E–09	1.25E–10	1.18E–10	3.66E–08
11	17.27	1.30E–08	20	30	6.50E–10	1.25E–10	1.05E–10	5.43E–08
12	17.27	1.00E–07	20	30	5.00E–09	1.25E–10	1.22E–10	6.32E–08
13	17.27	5.31E–08	20	30	2.66E–09	1.25E–10	1.19E–10	6.19E–08
14	17.27	4.47E–09	20	30	2.24E–10	1.25E–10	8.02E–11	4.15E–08

Table A1-16. Geometry and conductivity for shaft S4 when the grouting K = 1E–9 is applied to the walls of the shafts.

Calculation layer	Circumference, m	Kh, m/s	Dx, m	Thickness of calulation layer, m	Lc_aq, s^{-1}	LC_shaft, s^{-1}	Lc_tot, s^{-1}	Conductance, m^2/s
1	7.85	8.86E–06	20	1.7	4.43E–07	1.25E–10	1.25E–10	1.67E–09
2	7.85	1.30E–05	20	1	6.50E–07	1.25E–10	1.25E–10	9.81E–10
3	7.85	1.01E–06	20	1	5.05E–08	1.25E–10	1.25E–10	9.79E–10
4	7.85	1.01E–06	20	1	5.05E–08	1.25E–10	1.25E–10	9.79E–10
5	7.85	1.01E–06	20	4	5.05E–08	1.25E–10	1.25E–10	3.92E–09
6	7.85	1.01E–06	20	4	5.05E–08	1.25E–10	1.25E–10	3.92E–09
7	7.85	1.01E–06	20	4	5.05E–08	1.25E–10	1.25E–10	3.92E–09
8	7.85	7.38E–07	20	4	3.69E–08	1.25E–10	1.25E–10	3.91E–09
9	7.85	1.15E–07	20	11.5	5.75E–09	1.25E–10	1.22E–10	1.10E–08
10	7.85	3.10E–08	20	18	1.55E–09	1.25E–10	1.16E–10	1.63E–08
11	7.85	7.97E–10	20	30	3.99E–11	1.25E–10	3.02E–11	7.12E–09
12	7.85	2.14E–08	20	30	1.07E–09	1.25E–10	1.12E–10	2.64E–08
13	7.85	5.52E–08	20	30	2.76E–09	1.25E–10	1.20E–10	2.82E–08
14	7.85	4.04E–08	20	30	2.02E–09	1.25E–10	1.18E–10	2.77E–08

Table A1-17. Geometry and conductivity for shaft S5 when the grouting K = 1E–9 is applied to the walls of the shafts.

Calculation layer	Circum-ference, m	Kh, m/s	Dx, m	Thickness of calulation layer, m	Lc_aq, s^{-1}	LC_shaft, s^{-1}	Lc_tot, s^{-1}	Conductance, m^2/s
1	10.99	1.06E–06	20	1	0.000000053	1.25E–10	1.25E–10	1.37E–09
2	10.99	1.01E–06	20	1	5.05E–08	1.25E–10	1.25E–10	1.37E–09
3	10.99	1.01E–06	20	1	5.05E–08	1.25E–10	1.25E–10	1.37E–09
4	10.99	1.01E–06	20	1	5.05E–08	1.25E–10	1.25E–10	1.37E–09
5	10.99	1.01E–06	20	4	5.05E–08	1.25E–10	1.25E–10	5.48E–09
6	10.99	1.01E–06	20	4	5.05E–08	1.25E–10	1.25E–10	5.48E–09
7	10.99	1.01E–06	20	4	5.05E–08	1.25E–10	1.25E–10	5.48E–09
8	10.99	1.01E–06	20	4	5.05E–08	1.25E–10	1.25E–10	5.48E–09
9	10.99	1.05E–07	20	13.1	5.25E–09	1.25E–10	1.22E–10	1.76E–08
10	10.99	1.92E–09	20	18	9.6E–11	1.25E–10	5.43E–11	1.07E–08
11	10.99	2.18E–09	20	30	1.09E–10	1.25E–10	5.82E–11	1.92E–08
12	10.99	2.30E–07	20	30	1.15E–08	1.25E–10	1.24E–10	4.08E–08
13	10.99	2.89E–07	20	30	1.445E–08	1.25E–10	1.24E–10	4.09E–08
14	10.99	2.48E–07	20	30	1.24E–08	1.25E–10	1.24E–10	4.08E–08

Table A1-18. Geometry and conductivity for shaft S6 when the grouting K = 1E–9 is applied to the walls of the shafts.

Calculation layer	Circum-ference, m	Kh, m/s	Dx, m	Thickness of calulation layer, m	Lc_aq, s^{-1}	LC_shaft, s^{-1}	Lc_tot, s^{-1}	Conductance, m^2/s
1	17.27	3.00E–05	20	1	1.50E–06	1.25E–10	1.25E–10	2.16E–09
2	17.27	3.81E–05	20	1	1.91E–06	1.25E–10	1.25E–10	2.16E–09
3	17.27	4.00E–05	20	3.8	2.00E–06	1.25E–10	1.25E–10	8.20E–09
4	17.27	3.00E–06	20	1	1.50E–07	1.25E–10	1.25E–10	2.16E–09
5	17.27	1.11E–06	20	4	5.55E–08	1.25E–10	1.25E–10	8.62E–09
6	17.27	1.01E–06	20	4	5.05E–08	1.25E–10	1.25E–10	8.61E–09
7	17.27	5.76E–06	20	4	2.88E–07	1.25E–10	1.25E–10	8.63E–09
8	17.27	4.28E–08	20	4	2.14E–09	1.25E–10	1.18E–10	8.16E–09
9	17.27	4.28E–08	20	2.2	2.14E–09	1.25E–10	1.18E–10	4.49E–09
10	17.27	9.20E–08	20	18	4.60E–09	1.25E–10	1.22E–10	3.78E–08
11	17.27	6.48E–08	20	30	3.24E–09	1.25E–10	1.20E–10	6.24E–08
12	17.27	6.10E–08	20	30	3.05E–09	1.25E–10	1.20E–10	6.22E–08
13	17.27	1.07E–07	20	30	5.35E–09	1.25E–10	1.22E–10	6.33E–08
14	17.27	1.07E–07	20	30	5.35E–09	1.25E–10	1.22E–10	6.33E–08